UNIVERSIDADE DE SÃO PAULO
FACULDADE DE ODONTOLOGIA DE BAURU

BRUNNA MOTA FERRAIRO

Nanoparticulation methods of bovine hydroxyapatite, synthesis and structural/chemical characterization of an experimental SiO_2/nano-hydroxyapatite composite ceramic

BAURU
2020

BRUNNA MOTA FERRAIRO

Nanoparticulation methods of bovine hydroxyapatite, synthesis and structural/chemical characterization of an experimental SiO_2/nano-hydroxyapatite composite ceramic

Métodos de nanoparticulação da hidroxiapatita bovina, síntese e caracterização estrutural/química de um compósito cerâmico de SiO_2/nano-hidroxiapatita experimental

Tese constituída por artigos apresentada a Faculdade de Odontologia de Bauru - Universidade de São Paulo para obtenção do título de Doutor em Ciências no Programa de Ciências Odontológicas Aplicadas, na área de concentração Reabilitação Oral.

Orientador: Prof. Dr. José Henrique Rubo

Coorientadora: Profª. Drª. Ana Flávia Sanches Borges

Versão Corrigida

BAURU
2020

Ferrairo, Brunna Mota
Nanoparticulation methods of bovine hydroxyapatite, synthesis and structural/chemical characterization of an experimental SiO2/nano-hydroxyapatite composite ceramic/ Brunna Mota Ferrairo. -- Bauru, 2020.
81 p. : il. ; 31 cm.

Tese (doutorado) -- Faculdade de Odontologia de Bauru, Universidade de São Paulo, 2020.

Orientador: Prof. Dr. José Henrique Rubo

Nota: A versão original desta tese encontra-se disponível no Serviço de Biblioteca e Documentação da Faculdade de Odontologia de Bauru – FOB/USP.

FOLHA DE APROVAÇÃO

DEDICATÓRIA

Dedico este trabalho...

À **Deus**, que em sua infinita graça me conduz, protege e ampara. Desde a infância sou devota de Santa Terezinha e em uma de suas cartas encontra-se uma frase que é muito significativa para mim: "Nada acontece que Deus não tenha previsto desde toda a eternidade." Existem momentos na vida em que não existe mais ninguém, só você e Deus; e sou infinitamente grata à Ele por nunca estar verdadeiramente sozinha neste mundo.

À minha amada mãe, **Rosangela Fidelis da Mota Ferrairo**, mulher de fibra e de fé! A pessoa que me ensina todos os dias pelo exemplo: exemplo de mulher, de professora, de resiliência e de vida. Sua capacidade de amar tem um poder transformador e me faz acreditar que para tudo existe uma solução. Obrigada por fazer dos meus sonhos os seus e por nunca desistir; um passinho por dia chegamos ao longe. Te amo infinitamente e a ti dedico esta e todas as realizações da minha vida.

À minha **família**. Muitos acreditam em sorte, eu acredito em família! Se posso desfrutar do privilégio de viver meus sonhos e concluir minha faculdade e pós-graduação, é porque os tenho ao meu lado. A família é a raiz de quem somos, representa o amor que recebemos e a alegria do que vivemos. Todos os dias agradeço a Deus pelo maior presente que Ele poderia me dar. Amo vocês!

À minha coorientadora, **Profa. Dra. Ana Flávia Sanches Borges**, que idealizou e oportunizou a realização deste sonho. Com sua generosidade tive experiências ímpares e superei meus limites. Seu exemplo me fez compreender que a ciência vai muito além do "nosso mundinho" e quanto mais nos desafiamos, maior será a nossa realização profissional e pessoal. Obrigada pela amizade e carinho, por me deixar fazer parte da família TRATEBIO e por fomentar todos os dias o meu amor pela ciência.

Ao meu orientador, **Prof. Dr. José Henrique Rubo**, responsável pelo meu amor à disciplina de Prótese Dentária desde o meu segundo ano da graduação. Minha admiração pela sua competência, postura, generosidade, tranquilidade, senso de humor e ética é imensurável e só aumentou quando me tornei docente. Dizem que com o passar dos anos de pós-graduação nos tornamos cópias dos nossos orientadores. Sempre me alegro ao ouvir este ditado; se um dia eu for um terço do que o senhor é terei chegado muito além dos meus sonhos. Obrigada por todos estes anos de convivência e aprendizado, é uma honra ser sua aluna e orientada.

AGRADECIMENTOS

Aos meus Padrinhos, **Rosa Maria da Mota Moraes e Hildebrando Paulino de Moraes**, exemplos de perseverança, trabalho, fé e dedicação à família. São o alicerce da nossa casa e me provam todos os dias que nada supera a graça de termos uma boa família nos esperando em casa. O tamanho do meu amor por vocês só se compara à minha gratidão.

À minha tia, **Roseli Aparecida da Mota**, por seu amor, generosidade e zelo. Ao passo que se dedica inteiramente por amor ao próximo, és um símbolo de independência, garra e autenticidade como poucas pessoas conseguem ser. A senhora foi meu esteio nos piores dias da minha vida e seu carinho fez com que qualquer obstáculo fosse suportado e superado. Obrigada por tanto, te amo.

Ao meu namorado e melhor amigo, **Gabriel Abib Soriano**, pela paciência, carinho e companheirismo incondicional ao longo destes dez anos. Obrigada por me inspirar com a sua capacidade de superação, força e dedicação, por acreditar em mim e por estar ao meu lado nos momentos mais importantes da minha vida. Certamente você tornou o caminho mais prazeroso, leve e repleto de amor.

Aos meus primos/irmãos: **Patrícia da Mota Moraes, Priscila da Mota Moraes, Guilherme Ferrairo e Hildebrando Paulino de Moraes Junior** *(in memorian)*. Existe um pedaço de cada um de vocês em quem eu sou e a distância ou o tempo não são obstáculos para o nosso carinho e amor. Amo vocês!

Aos meus primos/sobrinhos, **Murilo Ferrairo e Olivia Moraes D'Andréa**. Há 15 anos atrás ganhei um companheiro para vida toda, somos muito parecidos e ao mesmo tempo muito diferentes. Lilo, obrigada por toda felicidade que me proporciona e por me ensinar tanto com seu carinho, inteligência e amor. Os anos se passaram, o amor da família se multiplicou e a menina mais esperta, criativa, engraçada e amorosa chegou. Olivinha, obrigada por trazer cores e sorrisos aos meus dias. É muito lindo poder acompanhar a descoberta do mundo e a construção de memórias... Amo vocês imensamente.

Aos amigos que me acompanham desde a graduação, **Gabriela Moura Chicrala, Felícia Miranda, Daísa Guerreiro Bernardes** e **Guilherme Toyoshima**. Obrigada por estarem ao meu lado em todos os momentos, por se fazerem presentes mesmo durante a correria do dia-a-dia e estando em jornadas tão distintas. É reconfortante quando nos encontramos e vejo que nada mudou, parece que nos vimos ontem.

Aos amigos que a pós-graduação me presenteou, **Ernesto Byron Benalcazar Jalkh, Natália Almeida Bastos, Samira Sandy Ferreira Strelhow, Gabriela de Araújo Lima, Ana Carolina da Silva Pinto, Pedro Hernandes Job** e **Jefferson Freire Cardoso.** Os desafios deste período são inúmeros e ter com quem dividir experiências, alegrias e tristezas, pacientes, seminários, artigos e momentos de lazer, sem dúvida nenhuma, foi uma grande benção. Obrigada por todo o carinho e companheirismo.

Aos amigos adquiridos com a experiência em docência, **Heliton Gustavo de Lima, Fernando Isquierdo de Souza, Sibelli Olivieri Parreiras, Andres Felipe Cartagena Molina, Gabriela Cristina de Oliveira, Mariana Midori**

Nagata, Willian Ricardo Pires e **Rafael Ferreira**, vocês são exemplos de dedicação e profissionalismo, tenho muito orgulho de ser amiga de jovens professores tão comprometidos com a ciência e a educação. Obrigada por tornarem os dois anos de UENP mais felizes e por permanecerem até hoje em minha vida.

As integrantes do time de orientadas do Professor Rubo, **Fernanda Ferruzzi Lima, Fernanda Furtado Piras, Milena Steluti Marques** e **Bárbara Margarido Brondino**, por dividirem trabalhos, risadas e tornarem estes sete anos de pós-graduação mais leves e frutíferos.

Aos amigos e companheiros de pesquisas e viagens, **Victor Mosquim** e **Lucas José de Azevedo Silva.** Victor, eu te admiro desde o primeiro dia que te conheci e este sentimento só aumentou conforme tive a oportunidade de convivermos. Lucas, você me ensina todos os dias com a sua dedicação e seu espírito leve. Obrigada por toparem qualquer desafio, por nunca abandonarem o barco e por me provarem que sempre cabe mais uma tarefa na agenda de quem se dedica totalmente a realização dos seus sonhos.

Aos integrantes do TRATEBIO – Translational Team for Biomaterials: **Prof. Dr. Paulo Noronha Lisboa Filho, Prof. Dr. Carlos Alberto Fortulan, Prof. Dr. Aroldo Geraldo Magdalena** e **Prof. Dr. David Santos Souza Padovini.** Com vocês aprendi que a ciência é como um prisma; cada área dará a sua contribuição, os conhecimentos se somarão e só assim nascerá o verdadeiro "eureka". Agradeço a paciência ao transmitir tanto conhecimento, a receptividade que sempre me receberam e o comprometimento com o trabalho, me espelho na generosidade de todos vocês.

Aos grandes professores que me inspiraram como docentes, pesquisadores e cirurgiões-dentistas: **Profa. Dra. Daniela Rios, Prof. Dr. Heitor Marques Honório, Profa. Dra. Linda Wang, Prof. Dr. Marco Antonio Hungaro Duarte, Prof. Dr. Estevam Augusto Bonfante, Profa. Dra. Karin Hermana Neppelenbroek** e **Prof. Dr. Paulo Francisco Cesar.** Muito obrigada pelos ensinamentos e por serem bons exemplos, provando que vale a pena trabalhar com quê se ama.

Aos professores orientadores da Clínica da Pós-graduação em Reabilitação Oral: **Prof. Dr. Luiz Fernando Pegoraro** e **Prof. Dr. Accácio Lins do Valle**. De vocês recebi inúmeras oportunidades e ensinamentos que sem dúvida nenhuma me tornaram uma melhor protesista, professora e, principalmente, ser humano. Obrigada pela generosidade, paciência, perseverança e pelo amor com que se dedicaram às atividades da pós-graduação.

Ao **Departamento de Prótese da FOB/USP**, representado pela Profa. Dra. Ana Lúcia Pompéia Fraga de Almeida, fazendo-se membro junto aos professores doutores: Paulo César Rodrigues Conti, Carlos dos Reis Pereira de Araujo, Estevam Augusto Bonfante, Gerson Bonfante, Karin Hermana Neppelenbroek, Lucimar Falavinha Vieira, Pedro César Garcia de Oliveira, Renato de Freitas, Simone Soares, Vinícius Carvalho Porto e Wellington Cardoso Bonachela. Agradeço por confiarem em mim e por compartilharem seus conhecimentos.

À secretária do Departamento de Prótese **Déborah Andrea Riêra Blasca**, por toda paciência, dedicação e simpatia. Aos funcionários: **Cleide Vital Martins, Marcelo Henrique G. de Sousa, Reivanildo F. Viana, Valquíria F. Nogueira** e **Ziley Mara Calepso de Castro**, pela atenção e solicitude.

À querida amiga, **Hebe Joselina de Freitas Pereira**, que não mede esforços para que a clínica de pós-graduação aconteça. Suas risadas e abraços apertados tornavam qualquer dia de atendimento mais leve. Ao técnico de laboratório **Alcides Urias da Costa**, uma pessoa com coração sem igual, sempre disposto a ensinar, ajudar e facilitar o nosso dia-a-dia com as pedras que surgissem pelo caminho. Às secretárias **Ana Letícia Polombo Momesso, Leila Regina da Silva Yerga Sanchez** e **Fátima Cassador Carvalho** *(in memorian)*, por toda presteza e carinho com os alunos.

À **Faculdade de Odontologia de Bauru**, Universidade de São Paulo, na pessoa do seu Diretor **Prof. Dr. Carlos Ferreira dos Santos**, a quem tenho profunda admiração como educador, pesquisador e gestor. Passei pelo portão da FOB em 2010 e após aquele instante minha vida nunca mais foi a mesma; tive os melhores professores, desfrutei da melhor estrutura, recebi o melhor suporte dos colaboradores técnico-administrativos, me apaixonei pela pesquisa e tive o privilégio de ser bolsista, vivi momentos inesquecíveis em atividades de extensão e, com isso, me formei profissionalmente em uma base sólida. Esta será minha segunda casa para sempre, não consigo mensurar meu orgulho e minha gratidão.

Aos **alunos da Faculdade de Odontologia de Bauru**, por me oportunizarem muito aprendizado ao acompanhá-los durante os laboratórios e as clínicas. Obrigada pela paciência e pelo carinho.

À **Universidade Estadual do Norte do Paraná**, na pessoa da sua Magnífica Reitora Fátima Aparecida da Cruz Padoan, por me receber como Professora Temporária no curso de Odontologia por dois anos. Obrigada pela confiança e oportunidade de ser a primeira professora de Prótese Dentária e, juntamente com

os professores doutores Fernando Isquierdo de Souza e Andres Felipe Cartagena Molina, estruturar a disciplina do zero. Foi um grande desafio e proporcional aprendizado.

Aos **alunos da Universidade Estadual do Norte do Paraná,** meus primeiros alunos e protagonistas na realização do meu sonho de ser professora. Cada um de vocês morará para sempre no meu coração. Sou extremamente realizada por ter conseguido plantar a sementinha do amor pela Odontologia e pela Prótese Dentária.

Aos **pacientes** que pude acompanhar durante esta trajetória. Obrigada pela generosidade, compreensão e colaboração.

À **Coordenação de Aperfeiçoamento de Pessoal de Nível Superior (CAPES)** pela bolsa de Doutorado, auxílio indispensável para a realização deste trabalho. E à **Fundação de Amparo à Pesquisa do Estado de São Paulo (FAPESP)**, pelo financiamento desta pesquisa – Processo 2018/23639-0.

Aos **professores integrantes da banca examinadora**, por terem dedicado seu tempo analisando, arguindo e contribuindo para a otimização deste trabalho.

A todos que contribuíram para que esta etapa tão importante da minha vida fosse concluída, o meu sincero obrigada!

"A ciência não é apenas uma disciplina de razão,

mas de romance e paixão"

Stephen William Hawking

RESUMO

Métodos de nanoparticulação da hidroxiapatita bovina, síntese e caracterização estrutural/química de um compósito cerâmico de SiO_2/nano-hidroxiapatita experimental

Objetivos: O objetivo deste trabalho foi testar dois métodos de nanoparticulação de hidroxiapatita bovina (HA), sintetizar um compósito cerâmico experimental SiO_2/nano-hidroxiapatita e caracterizá-los estrutural e quimicamente.

Materiais e Métodos: Corticais de fêmures bovinos foram selecionadas e, após a remoção da matéria orgânica, calcinadas e particuladas. Para realização da nanoparticulação dois métodos foram selecionados: sonicação e moagem por moinho de bolas. A sonicação foi realizada com 40 % da amplitude máxima de 750 W e 20 Hz em solução aquosa acrescida de HA e poliacrilato de amônia (4 h de ativação). A técnica de moagem utilizou um jarro de polietileno (300 cm^3) carregado com 40 vol% (500 g) de elementos de moagem (esferas de zircônia 3Y, HA, álcool isopropílico e ácido para-aminobenzóico), acoplados ao moinho rotatório (104 rpm, 48 h) seguido de moinho vibratório (72 h). Os produtos das técnicas de nanoparticulação foram caracterizados e a técnica de moagem foi utilizada para a síntese do compósito cerâmico experimental contendo sílica pirogênica e nano-HA de origem óssea bovina (SH). Os grupos foram conformados por compressão uniaxial/isostática, divididos em 3, 5 e 10 % de adição de HA, 1,2 e 2,4 % em peso de PVB e sinterizados à 1100, 1200 e 1300 °C para temperaturas máximas do platô (4 h). As caracterizações tanto dos métodos de nanoparticulaçõa, quanto do compósito cerâmico experimental foram realizadas por Microscopia Eletrônica de Transmissão (MET), Microscopia Eletrônica de Varredura (MEV), Espectroscopia de Energia Dispersiva de Raios-X (EDX), Difração de Raios-X (DRX) e Infravermelho por Transformada de Fourier (FTIR).

Resultados: O tamanho inicial das partículas de HA foram em média 75 μm e após as técnicas de sonicação e moinho de bolas foram de 60 nm e 40 nm, respectivamente. Ambas metodologias associadas à calcinação prévia, foram capazes de produzir partículas nanométricas de HA bovina, mantendo a estequiometria, morfologia e pureza adequadas. Com relação ao compósito cerâmico experimental SH, a compressão do pó foi um método eficiente. A temperatura de 1200 °C apresentou ligações químicas potencializadas sem a degradação do HA no perfil DRX. As imagens de MEV sugerem que 2,4 % em peso de PVB resultaram em

uma melhor compactação e menor incidência de trincas e poros, e a proporção de 5 % de HA apresentou propriedades potencialmente superiores para o biomaterial.
Conclusões: A técnica do moinho de bolas giratório e vibratório proporcionou uma maior redução das partículas de HA bovina e o compósito cerâmico experimental SH com 5 % de HA, 2,4 % em peso de PVB e sinterizado a 1200 °C apresentou propriedades potencialmente superiores para o biomaterial.

Palavras-chave: Cerâmica. Hidroxiapatita. Sílica. Cerâmica composta.

ABSTRACT

Nanoparticulation methods of bovine hydroxyapatite, synthesis and structural/chemical characterization of an experimental SiO2/nano-hydroxyapatite composite ceramic

Objectives: The aim of the study was to evaluate two methods of nanoparticulation methods of bovine hydroxyapatite (HA), synthesize an experimental SiO_2/nano-hydroxyapatite composite ceramic and made a structurally and chemically characterization of them.
Materials and Methods: Cortical of bovine femurs were selected and, after a pre-treatment, calcined and particulate. Sonication was performed with 40% of the maximum amplitude of 750W and 20Hz in aqueous solution added with HA and ammonia polyacrylate (4h of activation). Milling technique used a polyethylene jug (300 cm3) loaded with 40vol% (500g) milling elements (3Y zirconia balls, HA, isopropyl alcohol and para-aminobenzoic acid), placed in a rotatory mill (104rpm, 48h) followed by a vibratory mill (72h). Ball mill technique was used to mixture fumed silica and nano-HA from bovine bone source. Groups were divided into 3, 5 and 10% of HA addition, 1.2 and 2.4 wt.% of PVB, and 1100, 1200 and 1300 °C for maximum temperatures to firing plateau (4h). Characterization was performed by Transmission Electron Microscopy (TEM) / Scanning Electron Microscopy (SEM), Energy Dispersive X-ray Spectroscopy (EDX), X-ray Diffraction (XDR) and Fourier Transform Infrared (FTIR).
Results: The initial particle size is 75µm and sonication (60 nm) and ball mill (40 nm) techniques, associated with prior calcination, were capable of producing nanosized bovine HA particles, maintaining an appropriate stoichiometry, morphology and purity. According to SH composite ceramic, the uniaxial/isostatic powder compression is an efficient method. The temperature of 1200 °C presented potentialized chemical bonds without the degradation of HA at XDR profile. SEM images suggests that 2.4 wt.% of PVB result in optimized compaction and a lower incidence of cracks and pores, and the SH composite ceramic with 5% of HA presents potential superior properties to biomaterial.
Conclusion: The ball mill technique provided smaller particles of bovine hydroxyapatite and the experimental material SH composite ceramic with 5% of HA, 2.4 wt.% of PVB and sintered at 1200 °C presents potential superior properties to biomaterial.

Keywords: Ceramics. Hydroxyapatite. Silica. Composite Ceramic.

TABLE OF CONTENTS

1 INTRODUCTION

1 INTRODUCTION

Biomaterials can be defined as any nondrug individual or combined substance from synthetic or natural origin, which can be used any time, as a whole or as part of a system that treats, augments, or replaces any tissue, organ or function of the body [OLADEJI; UMORU; ARIBO, 2012; VON RECUM; LABERGE, 1995]. Historically, the humanity uses materials that are capable of being in contact with body fluids and tissues for long periods, whilst eliciting little, if any adverse reactions [DOREMUS, 1992]. In ancient Egypt, the first records of their use were found. Coconut shells for repairing injuries to skulls and animal tendons for sutures are some examples [DSM, 2009]. The ideal biomaterial must present nonimmunogenic, biocompatibility, bioresorbable, and biodegradability properties. There is a high demand in research for those suitable for restorations and bone tissue replacement [HENCH; POLAK, 2002].

Applicability also will depend on the mechanical, physical, structural, and chemical properties. In general, biomaterials are commonly used as implants [DENISSEN *et al.*, 1989], tissues and organ transplants [ZHOU; LEE, 2011], and in drug delivery systems [MONDAL; DOROZHKIN; PAL, 2011; SZCZE; HO; CHIBOWSKI, 2017]. There is a wide variety and they can be classified in three main forms: (1) according to the origin {biological (autogenous, allogeneic or xenogenous) or synthetic/alloplastic (metals, polymers and ceramics)}, (2) to the response induced to the environment (bioinert, bioabsorbable or bioactive), and (3) according to generation {first / bioinert, second / bioactive and biodegradable or third-generation / stimulators of cellular responses at molecular levels (biomimetics and tissue engineering)}. Noticing that the classification by generations must not be interpreted chronologically, but conceptually [HENCH; POLAK, 2002].

Among the biomaterials, bioceramics have great prominence for bone replacement because of the potential of body interaction which reflects into promotion of tissues regeneration, helping the healing and restoring physiological functions [OLADEJI; UMORU; ARIBO, 2012]. Since then, bioceramics have been proposed for biomedical and dental applications and are divided into “bioinert” high strength ceramics (e.g., alumina, zirconia), bioactive ceramics (e.g., hydroxyapatite, bioglass, glass ceramic), and various bioresorbable ceramics with active surface in metabolic processes with predictable results (i.e. tricalcium phosphate) [VON RECUM; LABERGE, 1995].

A noticeable representative of bioactive ceramics is the hydroxyapatite (HA). With $Ca_{10}(PO_4)_6(OH)_2$ as its general formula [DE JONG, 1926], is the main mineral component of bones and teeth, being responsible for its hardness and strength. This biomaterial is of great interest in many fields due to its remarkable structure and inherent properties. Considered to be an environment-friendly material, HA presents excellent biocompatibility, non-toxicity, osteoconductive property, nondregadability, noncarcinogenic and nonimmunogenic reactions, and good hemocompatibility, optimizing the applicability in bone tissue regeneration [ZHOU; LEE, 2011] and drug delivery system [MONDAL; DOROZHKIN; PAL, 2018]. The chemical and thermal stability of HA remains the major reasons that make it an attractive material choice and an excellent candidate for biomedical applications [FU *et al.*, 2016; FULLER *et al.*, 2002]. Other physicochemical properties of HA are also relevant and make it a very promising candidate for applications beyond health. The use of HA on treatment of air, water and soil pollution is possible due to the absorption capacity and ion exchange capability which contribute to the retention and removal of pollutants, facilitating the catalytic activity of heterogeneous surfaces [IBRAHIM *et al.*, 2020], being effective even in the recovery of nuclear waste [FULLER *et al.*, 2002].

There are two main methods for HA obtainment; inorganic synthesis such as sol-gel, hydrothermal, emulsion, hydrolysis, combustion, pyrolysis, solid-state and mechanochemical methods [SADAT-SHOJAI *et al.*, 2013], or from biological sources or wastes such as mammalian bone, marine or aquatic sources, shells, plants or even mineral sources [MOHD PU'AD *et al.*, 2013]. Is inevitable the comparison between methods and, although many synthesis methods have been developed, the obtainment of HA without formation of toxic intermediary products still remains a challenge. Natural HA is non-stoichiometric presenting trace elements that mimics the apatite produced from human bone and accelerate the process of bone formation [AKRAM *et al.*, 2013], despite the deficit in calcium and phosphorus [BOSKEY, 2013].

Among the peculiarities of HA from natural sources, its sustainable and economic appeal is highlighted [AKRAM *et al.*, 2013]. The ability to combine excellent chemical and biological properties with sustainability, environmentally friendly and economy is remarkable. Bovine bone is a good source of natural HA because of the morphological and structural similarity to human's bone, specially the cortical of the femoral bone [HERLIANSYAH *et al.*, 2007]. Properties such as size, shapes and crystalline phases of Ca/P and CA/P ratio, differ according to extraction and calcination methods [MOHD PU'AD *et al.*, 2013]. A pretreatment is preconized to initiate the removal of organic components and calcination complete it,

eliminating eventual pathogens presented [AKRAM *et al.*, 2013; RUKSUDJARIT *et al.*, 2008]. The use of additional methods helps to reduce the size of HA particles and optimize its properties.

The nanosized HA (grain size ≤ 100 nm) with appropriate stoichiometry, morphology and purity presents optimized surface activity and similarity to mineral found in hard tissue [VALLET-REGÍ; GONZÁLEZ-CALBET, 2004]. Although there are several nanoparticulation methods, synthesize a well-defined powder for a specific application is laborious and essential to evaluate their accuracy in controlling stoichiometry, crystallinity, geometry, size and size distribution, and degree of particle agglomeration [MOHD PU'AD *et al.*, 2019]. Wet methods have the ability to control the morphology and the mean size of powder, however, the medium solution can be incorporated into the crystal structure, leading impurities, and the low preparation temperature results in lower crystallinity and Ca/P phases different than HA [MOHD PU'AD *et al.*, 2019]. Sonochemical synthesis uses the acoustic cavitation in an aqueous phase where the collapse of microbubbles occurs [JEVTIC, M. *et al.*, 2008] and promote a rise if HA crystal growth up to 5.5 times with more uniform [ROUHANI; TAGHAVINIA; ROUHANI, 2010]], smaller, purer crystals with minimal agglomeration [ROUHANI; TAGHAVINIA; ROUHANI, 2010; CAO; ZHANG; HUANG, 2005; GIARDINA; FANOVICH, 2010]. Classified as mechanochemical method, the effect of planetary mill or ball mill vary according to the milling medium, type and diameter of the milling balls, atmosphere, steps and pauses, duration, speed and the powder-to-ball mass ratio [HONARMANDI *et al.*, 2010; YEONG; WANG; NG, 2001; KRAJEWSKI *et al.*, 1996]. Although it is an effective method, caution is necessary because long milling time leads to decrease in a crystallite size and increase in lattice strain and crystallinity [NASIRI-TABRIZI; HONARMANDI; EBRAHIMI-KAHRIZSANGI, 2009].

Biomaterials based on nano-HA enhanced densification and sinterability [BOSE, S. *et al.*, 2009], improved cell differentiation and proliferation [WANG; LIU; GUO, 2010], decreased apoptotic cell death [CAI, Y. *et al.*, 2007], and enhances resorbability, bioactivity, osteointegration and bone tissue formation in comparison to micron-sized HA [DOROZHKIN, 2010]. These characteristics make possible their applicability on the most diverse domains of Dentistry. On prevention, nano-HA functions as dentinal hypersensitivity and remineralizing therapeutic element; on esthetics, as adjuvant material for bleaching therapy; and on surgery, implantology and periodontology they are used as coatings for titanium implants, it has remarkable properties as a sinus lifting material, superior bone regenerating properties

compared to autologous bone graft, and scaffolds [BORDEA, I.R. *et al.*, 2020]. In all applications, bioactivity is the most requested characteristic and its maximization is of great clinical interest.

Silica (SiO_2), or silicon, is an important micronutrient for bone and connective tissue health [CARLISLE, 1972; SCHWARZ; MILNE, 1972]. In bone, Silica (Si) is involved in early stages of bone mineralization stimulating osteoblast cells [CARLISLE, 1972]. The association of Si-HA was proposed aiming to maximize the bioactivity and presents favorable *in vivo* results [GIBSON; BEST; BONFIELD, 1999]. An initial cellular and ionic process occurs on their surface which allows the subsequent crystallization of apatite crystals, collagen formation and cell adhesion [PATEL *et al.*, 2002; HENCH; CLARKE, 1982]. The benefit of early bone ingrowth and repair is directly related to Si influence in cell proliferation ability and induction of osteogenic signal in human mesenchymal cells, that although transitory, it is considered significant [KRUSE *et al.*, 2011]. Although the association Si-HA has been much discussed, there is a gap in the literature regarding the densified conformation with silica matrix and HA acting as its additive. Sintering temperature, timing and atmosphere, starting powder grain size and shape, pressure, composition and preparation methods are some factors that influence dense ceramics preparation [TURNER, 2009; BOWEN; CARRY, 2002].

The synthesis of a new biomaterial is classified as having a high innovative content, since it is part of the development based on unprecedented knowledge, and as highly complex, since associates different types of knowledge and multidisciplinary interaction. With the development of synthesis approaches, traditional materials as ceramics have been constantly redesigned and enhanced [WANG; CHOU; ZHANG, 2019]. A crucial stage of the innovation process is an extensively structural and chemical characterization by systematic methods. High-resolution scanning electron microscopy (SEM), scanning transmission microscopy (TEM), energy dispersive x-ray spectroscopy (EDX), x-ray diffraction (XDR), and Fourier transform infrared (FTIR) are some examples of method that may provide tools for exploring properties of innovative or existing biomaterials [BRANDON; KAPLAN, 2013]. The applicability study will continue the flow of investigation, directing its use based on its performance. This stage includes methods such as mechanical and optical tests, fractographic analysis, density, permeability, among others.

Seeking innovation, sustainability and development of intelligent materials, the aim of this study was to evaluate the effectiveness of two nanoparticulation methods of bovine HA and to synthesize an experimental SiO_2/nano-HA composite ceramic via uniaxial/isostatic powder compression. The hypotheses consist in the effectiveness of the grinding and sonication

processes to reduce HA particles on a nanometric scale and in obtaining an experimental biomaterial with promising chemical and structural characteristics for future clinical employability. Factors such as the variation in the addition of HA in SiO_2 matrix, concentration of binder, and different sintering temperatures were performed. Based on structural and chemical characterization, the effectiveness of the sonication and ball mill method in reducing HA particles and the microstructure of the new synthesized ceramic material was extensively analyzed giving support to the methodological originality presented by the study.

2 ARTICLES

2 ARTICLES

2.1 ARTICLE 1

Nanoparticulation of Bovine Hydroxyapatite by Sonochemical an Mechanochemical Ball Mill Methods: Physical and Chemical Characterization

This article was submitted to *Biomaterials* and was in accordance with this journal.

B. M. Ferrairo[1]; V. Mosquim[2]; L. A. Pires[2]; F. M. L. Pontes[3]; A. G. Magdalena[3]; C. A. Fortulan[4]; P. N. Lisboa-Filho[5]; A. F. S. Borges[1,2]*; J. H. Rubo[1].

[1] Department of Prosthodontics and Periodontics, Bauru School of Dentistry, University of São Paulo, Bauru, SP, Brazil.
[2] Department of Operative Dentistry, Endodontics and Dental Materials, Bauru School of Dentistry, University of São Paulo, Bauru, SP, Brazil.
[3] Department of Chemistry, UNESP - School of Science, São Paulo State University, Bauru, SP, Brazil.
[4] Department of Mechanical Engineering, São Carlos School of Engineering, University of São Paulo, São Carlos - SP, Brazil.
[5] Department of Physics, School of Sciences, São Paulo State University, Bauru - SP, Brazil.

***Corresponding author**: Ana Flávia Sanches Borges, Alameda Dr. Octávio Pinheiro Brisolla, 9-75, Vila Universitária, ZIP CODE: 17012-901. Bauru, São Paulo, Brazil. Telephone: +55 014 3235-8000. e-mail: afborges@fob.usp.br

Acknowledgments

This work was supported by the São Paulo Research Foundation (FAPESP), process number: 2018/23639-0. The authors would like to thank CAPES “Coordenação de Aperfeiçoamento de Pessoal de Nível Superior - Brasil - Finance Code 001".

ABSTRACT

The size and quality of the hydroxyapatite (HA) particles are crucial factors and can significantly increase their biocompatibility and bioactivity. This study aims to evaluate the effectiveness of sonochemical and milling nanoparticulate techniques using HA of bovine origin. The starting powder were characterized using X-ray diffraction (XRD), Fourier transform infra-red (FTIR), scanning electron microscopy (SEM), energy dispersive spectroscopy (EDS), and transmission electron microscopy (TEM) (75µm). Sonication was performed with 40% of the maximum amplitude of 750W and 20Hz in aqueous solution added with HA and ammonia polyacrylate (4h of activation). Milling technique used a polyethylene jug (300 cm^3) loaded with 40vol% (500g) milling elements (3Y zirconia balls, HA, isopropyl alcohol and para-aminobenzoic acid), placed in a rotatory mill (104rpm, 48h) followed by a vibratory mill (72h). After these processes, the same protocol of initial analyses were performed. The results reveal that the final average grain size of HA was 40 nm for milling technique and 60 nm for sonication (TEM). FT-IR showed a broad band at 1300-500 cm^{-1}, and similar peaks, without degradation of the HA bonds, regardless of the two forms of HA nanoparticulation. XDR analysis showed peaks equivalent to those in the literature for synthetic and animal HA. In addition, the equivalence between the methods peaks demonstrated the structural maintenance. The same chemical characteristics were also demonstrated in the samples from the EDX. It was concluded that both methods were able to decrease the particles without damaging them, but the milling method produced smaller particles.

Keywords: Ceramic material. Nanoparticles. Nanostructured materials. Hydroxyapatite.

Highlights:

- Biocompatibility and bioactivity are directly affected by the size and quality of the particles.
- It is necessary to reduce the particle without physicochemical degrading it.
- The sonochemical and grinding methods produced nano-HA without degradation.

INTRODUCTION

Hydroxyapatite ($Ca_{10}(PO_4)_6(OH)_2$, HA) is widely used for skeletal and dental reconstructions due to its excellent properties as biocompatibility, bioactivity, high osteoconduction and/or osteo-induction, nontoxicity, noninflammatory behavior and nonimmunogenicity [1 - 3]. Due to the delimited supply of autologous bone and its high applicability and consumption, the search for alternative sources is influenced.

The extraction of HA from biological resources, for example biogenic (eggshells, seashells and calcite materials), plants (bamboo, calendula flower, etc.) or bones (mammalian and fish bones) origins, are a safe and more balanced option from the sanitary, economic and environmental points of view to obtain the biomaterial [4, 5]. Moreover, the organic components and possible pathogens are eliminated during the calcination process, leaving only the mineral component with beneficial trace ions to speed up the bone formation process [6].

The nanoscale form can significantly increase the characteristics of biocompatibility and bioactivity of HA [7], since it presents a high ratio between surface area and volume, approaching in size and chemical composition to the human bone tissue [8]. Manipulating the material at the atomic and molecular level improves the mechanical stability of the bone frame and provides a more appropriate chemical surface and porosity for cell proliferation optimizing biocompatibility [9 - 11].

There are several methods of HA nanoparticulation. The main synthesis techniques can be grouped into dry methods, wet methods, processes at high temperatures, synthesis methods based on biogenic sources and the combination of them [5]. For this study, both combined methods were selected. An initial thermal step of calcination and after a representative of the dry methods (mechanochemical method) and one of the wet methods (sonochemical method) were selected. Both classified as low cost and with the ability to obtain nanometric particles with diverse morphology, different degrees of crystallinity, purity phase and Ca/P ratio [5].

It is of great interest not only to evaluate the particle size reduction capacity of the methods from biological resources, but also the quality from its physical and chemical properties, crucial aspects to achieve optimal properties. In this study, two main directions were followed; the first purpose was to reach the nanoscale reduction of HA particles from bovine origin in the different methods used. The other goal was to evaluate the effect of the methods on the particles, evaluating its physical and chemical characteristics in order to optimize their use. X-ray diffraction associated with Rietveld refinements, Fourier transform infrared spectra,

energy dispersive X-ray spectroscopy and transmission electron microscopy were used to investigate structural and morphological properties of the samples.

MATERIAL AND METHODS

Obtainment of HA

The extraction of HA from bovine bones aims at a sustainable approach; recovering and processing residues that would be discarded in landfills or used for the production of animal food. Bovine femurs had their organic matter removed by thermochemical process [12] (Fig. 1A) and were reduced with the aid of mortars and pestles (Fig. 1B). Samples were submitted to chemical and cytotoxic analyzes to verify the absence of heavy metals and biological contamination in the bone composition. Once the results were negative, the bones were released for use.

In order to obtain an uniform and submicrometric powder, the granules were milled in a jug of polyethylene (85 mm of height and 300 cm^3 of volume) loaded with 40% vol (500 g) of spheres of 3Y zirconia ∅ 3 mm making up a useful volume of 100 ml, para-aminobenzoic acid ($C_7H_7NO_2$) as deflocculant and isopropyl alcohol (C_3H_8O) as the solvent of the liquid medium binder solvent. The jar was filled with a concentration of 30% vol solids and placed in a gyratory mill (104 rpm for 48 hours) (Fig. 1C) followed by a vibratory mill (72 hours) (Fig. 1D). The samples were dried in an oven at 80 ºC and granulated in stainless steel sieves of # 200 mesh ≤ 75μm.

Initial characterization

X-ray diffraction (XRD) patterns characterizes the structural phase (Rigaku D/MAX 2500 PC with CuKα radiation source (λ = 1.54056 Å) with rotatory anode operation at 40 KV and 150mA). The Scherrer equation [26] was used to determine the crystallite size of the HA.

$$D = \frac{0.9\lambda}{\text{FWHM} \cdot \cos\theta}, \quad (1)$$

Where the crystallite size (nm), the wavelength is $\boldsymbol{\lambda}$ (0.0154056 nm), the full width at half maximum (FWHM) of the diffraction peak under consideration (rad) and the diffraction angle $\boldsymbol{\theta}$ (deg). The software “PANalytical X’Pert HighScore” and “PCPDFWIN” were used to propose standards and evaluate the XDR profiles by the Joint Committee on Powder Diffraction and Standards (JCPDS). The JCPDS involved card # 024-0033 for HA, # 009-0080 for $CaHPO_4$, # 001-1160 for CaO and # 001-0941 for $Ca_3(PO_4)_2$.

Fourier transform infrared (FT-IR) spectra were recorded (FTIR-Vertex 70, Bruker) with KBr pellets, in the transmittance mode with the range of 500-2500 cm^{-1}, in order to investigate the functional groups of resultant powders.

To semi-quantitative examination the energy dispersive X-ray spectroscopy (EDX) which was coupled with scanning electron microscopy (SEM, SERON AIS-2100) was performed. The samples were coated with gold at ≅ 10 nm thickness and were investigated using an XL30 FEG, an ultra-vacuum system with the base pressure of 1×10^{-5} Pa and an acceleration voltage of 20 kV.

As a further structural analysis based on exploring the individual nanostructures and to measure the initial particle size and agglomeration phenomenon, the transmission electron microscopy (TEM, Philips CM200) was performed at 200 kV. Samples were prepared by dropping a diluted suspension over a 300-mesh carbon coated copper grid drying the excess solution with a semi permeable paper. Images were obtained with the aim of identifying the crystallographic orientations and the crystallinity of the nanoparticles.

X-ray fluorescence analysis by wavelength dispersion (WDXRF) is also performed to verify if the chemical composition was in accordance with ASTM F1185-03, which determines the maximum concentration of heavy metals allowed for the HA obtained from animal origin.

Methods of nanoparticulation

In order to test the efficiency of particle decrease without degradation, two methods were selected.

A. Ball mill

Using a polyethylene jug (300 cm^3) loaded with 40vol% (500 g) milling elements (3Y zirconia balls, HA, isopropyl alcohol and para-aminobenzoic acid) placed in a ball mill (104 rpm, 48 h) and after in a vibratory mill (72 h), grinding was performed. After that, the alcohol was evaporated with the aid of a heated air blower (≅ 80 ºC) and the powder was granulated in stainless steel sieves of # 200 mesh ≤ 75μm.

B. Sonochemical

HA powder was submitted to ultrasonic processing in a Sonics brand model VCX-750, 750W of power and frequency of 20 kHz for 4 h, with pulses of 5 min and variable amplitude fixed up to 40% from the nominal amplitude of the equipment (750 W/cm^2). The Ca/P molar ratio was fixed at 1.67 and the concentration of Ca^{2+} ions was 0.02 M.

The choice of aqueous solution (deionized water - Milli-Q® systems) is due to its purity, avoiding contamination and chemical interaction during acoustic cavitation. Although its high vapor pressure (17.5 mmHg – 20 °C), samples were cooled with an ice bath and deionized water was added in order to leave the solution always in a constant volume and standardize the effect of acoustic cavitation.

To prevent agglomeration of the particles, ammonium polyacrylate deflocculant ($C_3H_4O_2$ - NHPA) was added to the mixture during the sonication (0.1 wt.%) [13]. After the process, the aqueous portion was dried in an oven at 80 ºC and granulated in stainless steel sieves of # 200 mesh ≤ 75μm.

Final characterization

Performed the nanoparticulation methods, samples in liquid medium were submitted to TEM, and dry samples were collected for XDR, FTIR and EDX.

RESULTS AND DISCUSSION

As important as decrease the particles size is the maintenance of an appropriate stoichiometry, morphology and purity [14]. Methods capable of controlling the geometry, size/distribution, crystallographic and chemical structure, reflects in great mechanical and in vitro and in vivo biological properties [5]. The combined methods have been frequently used and seems to improve the final properties of HA from natural sources [5]. For bovine bones the most frequent association is hydrothermal and calcination [34]. The present study demonstrates that the association between calcination and sonochemical or the ball mill also provide promising results of reaction kinetics, reduction of particle size and high purity.

The FTIR spectrum of the samples and the amplification of bands 1300 – 500 cm-1 are presented in Figure 2. A narrow band near 965 cm^{-1} represents the v1 mode of PO_4^{3-} ions apatite, present in all spectra of HA and carbonated apatites. The band at 469 cm-1 is assigned to the v2 phosphate mode in bending vibration and it does not appear in the spectrum. The v2 band of CO_3^{2-} is located at 873 – 880 cm^{-1} (out-of-plane bend vibration), this absorption results from out-of-plane stretching. The main signal of the phosphate group appears in the triply degenerate v3 domain (1100 – 1035 cm^{-1}). The v3 mode, between 1400 – 1600 cm^{-1}, is composed of two bands [15] and represents the strongest IR band for carbonate. Band at 700 cm^{-1} indicates C-O absorption, its combination with the v3 signal indicates that no calcite was associated with the HA [16]. The v4 phosphate mode will appear in different sites for carbonated apatite (bending

vibration); 633, 603 and 565 cm-1 bands [17, 18]. Frequently carbonate ions are associated with impurity, i.e., residual organic component after calcination [19]. Absorbed water (1635 cm-1 region) was almost imperceptible in spectra. The slight presence of the characteristic peak at 650 cm-1 (shift to 660 cm-1) due to v1(OH) in the HA could be better visualized using high energy transfer inelastic neutron scattering spectroscopy [20]. As important as the identification of the peaks presented is the relevant observation of their maintenance of shapes and intensities of the absorption band in FTIR spectra after performing the methods demonstrates, which demonstrates the methods preservation capacity.

The nanoparticulation methods did not present any complications during the performance. The white color, with some parts of light yellow, of the bovine bone powder indicates the beginning of organic matrix removal after thermochemical process with hydrogen peroxide (H2O2) as a 30 %, 100 volume aqueous solution, heated to 100 °C. Most literature report a pre-treatment which involves remove the fat, protein and soft tissues, and cut the bone into small pieces before boiling [30, 35, 36]. Caring for this previous process ensures that a larger surface area comes into contact with chemical agents and guarantees a good sample. The pre-treatment was completed after the calcination with a heating curve up (5 °C / minute) to 900 ºC, two-hour plateau [33] and long-term cooling temperature, uniformizing the white color, demonstrating that any remnants of protein and collagen, e.g., have been removed [21, 22]. The use of thermal method increases the crystallinity [4] and the proper temperature for HA from bovine bone sintering is around 1000 °C based on two-thirds of the melting point (2/3 x 1227 + 273) K [22]. High temperature results in degradation of the calcium phosphate, at 850 ºC β-tricalcium phosphate (β-TCP) starts to be obtained and at 900 and 1000 ºC the pure crystalline HA still can be produced [4]. Choosing 900 ºC ensures that partial dehydration will initiate, the production of β-TCP and a creeping reaction of hydroxides or carbonates to the respective oxides, avoiding the melting point of bovine bone as demonstrated in studies with differential thermal analysis (DTA) [22, 23, 24, 33]. Also, temperatures above 800 ºC are capable of eliminating all pathogens, preventing the possibility of diseases transmission [37].

XDR is a relevant technique to identify the phases before and after the nanoparticulation methods. Figure 3 shows XDR patterns, the resulting diffractogram demonstrates that data were in accordance with previously reported descriptions of the XDR structure and characteristic pattern of bovine origin HA (XDR JCPDS file no. 9-432, 1996) [25] and with pure HA phase [33]. The peaks intensity and the correspondence of (211), (300), and (202) diffraction peaks in precursor and after nanoparticulation methods HA powder highlight the production of pure HA nanoparticles. The strongest (211) peak at 31.9° corresponds to HA (P63/m) belonging to

the hexagonal symmetry (JCPDS 9-432). These results indicate the dihydroxylation of the HA and, as the hydroxyl carbonate apatite, is beneficial for biomedical purposes due to its similarity with the bone apatite [22]. The peak of all carbonated calcium hydroxyapatite (CHA) at (002) reflection was clearly broader. Characteristic peaks for $\boldsymbol{\beta}$-TCP which are located at $2\boldsymbol{\theta}$ angles of 27.75, 31.65, 45.55, and 48.00° that normally do not appear in samples calcined at temperature below a 1000°C are evident in both methods samples, although less intensely present. The shape of the XDR peaks suggests a well crystallized and the broadened nature implies that the grain sizes are on nanometer scale [16]. The estimative average grain size is 32.08 nm for sonochemical and 51.15 nm for ball mill method using the Debye-Scherrer formula, which was consistent with TEM method.

Bovine HA presents 93% $Ca_{10}(PO_4)_6(OH)_2$, 7% $Ca_3(PO_4)_2$ and $\boldsymbol{\beta}$-TCP as crystalline phase composition. The similarity to natural bone mineral is reported [22] and in this study the HA crystallized in the hexagonal space group P63/m. The EDX method allows qualitative and quantitative analysis of inorganic elements present in a sample and confirms the presence of Ca, P, and O (Figure 4). The properties of hydroxyapatite are strongly dependent on its stoichiometry, the reactivity of its surface and its biological behaviour. Thus, the Ca/P molar ratio is one of the ways used to characterize the composition of different calcium phosphates. A Ca/P ratio of ≅ 1.92 obtained fits with the acceptable range [27, 28] and appears to be a good candidate for bone substitute. HA extracted from the mammalian sources contains trace elements with optimum potential for enhancing the biological properties of natural HA, and they are not founded in other sources [4]. Examples of these minor elements are Mg^{2+} and Na^{+}, which appear in our EDX samples, and are the most frequently found.

TEM images provide the analyse of nanoparticle size and reveals the morphology of the HA samples. Figure 5 shows the TEM images from initial (a), sonochemical (b) and ball mill (c) HA samples. There are different forms of HA crystallites: needles, flakes, spheres, rods, and plate-like. The particles shape was not affected by the extraction method or source, and even the same source of bone could produce different shapes [4]. In our experiments, the aggregation resulted in nanoflakes with average size of ≅ 75 μm for initial samples, ≅ 60 nm for sonication, and ≅ 40 nm for ball mil technique (Figure 6), similar results were found by Ayatollahi et al [33]. Samples of the sonication technique showed difficulty in signalling diffraction. The presence of amorphous material around the nanoparticles can be suggested as a justification. Although, the sonochemical is a wet-chemistry method and the lattice parameters might have suffered with water inclusion and/or atypical surroundings [29]. The deflocculant polymer in aqueous medium encompassed the HA nanoparticle which hindered the diffraction and the

formation of the crystalline plane (Figure 5b). For the samples of the ball mill group in alcoholic medium there was no such event and the diffraction signal did not present any difficulty. There is a competition between the amorphous phase and the crystalline phase, however the sample has diffracted (Figure 5c). Further studies are necessary to variate and elucidate the interaction between deflocculant polymer, HA nanoparticle and the type of medium.

CONCLUSION

The present research has demonstrated the viability of nanoparticulation of bovine hydroxyapatite by sonication and ball mill methods, associated with prior calcination. The samples showed the maintenance of an appropriate stoichiometry, morphology and purity. Due to the increasing demand for nano-HA in biomedical application, its noticeable to elucidate methods that are capable of obtaining phase purity, thermal stability, low cost and from a sustainable source.

1- Bovine bone is a raw material and natural source suitable for obtaining nano-hydroxyapatite.

2- Sonication (≅ 60 nm) and ball mill (≅ 40 nm) methods were efficient for obtaining particles on a nanometric scale, indicated by TEM images and XDR analysis.

3- The XDR profile of both methods has a good coincidence with stoichiometric HA indicating a high crystallinity and a single phase of HA.

4- FTIR showed a broad band at 1300-500 cm^{-1}, and similar peaks, without degradation of the HA bonds, regardless the two forms of HA nanoparticulation.

5- The same chemical characteristics were also demonstrated in the samples from the EDX.

ACKNOWLEDGMENT

This work was supported by the São Paulo Research Foundation (FAPESP), process number: 2018/23639-0. The authors would like to thank CAPES “Coordenação de Aperfeiçoamento de Pessoal de Nível Superior - Brasil - Finance Code 001".

References

1. C.A. Stewart, Y. Finer Y, Biostable, antidegradative and antimicrobial restorative systems based on host-biomaterials and microbial interactions, Dent Mater. 35 (2019) 36-52. https://doi: 10.1016/j.dental.2018.09.0131. N.A.M. Barakat, M.S. Khil, A.M. Omran, F.A. Sheikh, H.Y. Kim, Extraction of pure natural hydroxyapatite from the bovine bones bio waste by three different methods, J. Mater. Process. Technol. April (2009) 209:3408-3415. https://doi.org/10.1016/j.jmatprotec.2008.07.040
2. J.C. Elliott, Structure and Chemistry of the Apatites and Other Calcium Orthophosphates, first ed., Elsevier, Amsterdam, 1994.
3. N.A.S. Mohd Pu'ad, P. Koshy, H.Z. Abdullah, M.I. Idris, T.C. Lee, Syntheses of hydroxyapatite from natural sources, Heliyon. (2019) May 8;5(5):e01588. https://doi.org/10.1016/j.heliyon.2019.e01588
4. M. Sadat-Shojai, M.T. Khorasani, E. Dinpanah-Khoshdargi, A. Jamshidi, Synthesis methods for nanosized hydroxyapatite with diverse structures, Acta Biomater. (2013) Aug;9(8):7591-621. https://doi.org/10.1016/j.actbio.2013.04.012
5. M. Akram, R. Ahmed, I. Shakir, W.A.W Ibrahim, R. Hussain, Extracting hydroxyapatite and its precursors from natural resources, J. Mater. Sci. 49 (2014) 1461–1475. https://doi.org/10.1007/s10853-013-7864-x
6. L. Chen, J.M. Mccrate, J.C.M. Lee, H. Li, The role of surface charge on the uptake and biocompatibility of hydroxyapatite nanoparticles with osteoblast cells, Nanotechnology (2011) 22:105708. https://doi.org/10.1088/0957-4484/22/10/105708
7. G.M. Raghavendra, K. Varaprasad, T. Jayaramudu, Chapter 2 - Biomaterials: design, development and biomedical applications, in: S. Thomas, Y. Grohens, N. Ninan (Eds.), Nanotechnology Applications for Tissue Engineering, William Andrew Publishing, Oxford, 2015, pp. 21–44.
8. A. Balamurugan, A.H.S. Rebelo, A.F. Lemos, J.H.G. Rocha, J.M.G. Ventura, J.M.F. Ferreira, Suitability evaluation of sol-gel derived Si-substituted hydroxyapatite for dental and maxillofacial applications through in vitro osteoblasts response, Dent. Mater. 24 (2008) 1374–1380. https://doi.org/10.1016/j.dental.2008.02.017
9. C. Capuccini, P. Torricelli, F. Sima, E. Boanini, C. Ristoscu, B. Bracci, G. Socol, M. Fini, I.N. Mihailesca, A. Bigi, Strontium-substituted hydroxyapatite coatings synthesized by pulsed-laser deposition: in vitro osteoblast and osteoclast response, Acta Biomater. 4 (2008) 1885–1893. https://doi.org/10.1016/j.actbio.2008.05.005

10. S.M. Rabiee, F. Moztarzadeh, M. Solati-Hashjin, Synthesis and characterization of hydroxyapatite cement. J. Mol. Struct. 969 (2010) 172–175. http://dx.doi.org/10.1016/j.molstruc.2010.01.068
11. R. Erbelli, Avaliação da qualidade óssea de bovinos. Dissertação (Mestrado em Bioengenharia) - Bioengenharia, Universidade de São Paulo, São Carlos (2017). doi:10.11606/D.82.2018.tde-20082018-121530.
12. B.D. Cullity, S.R. Stock, Elements of X-Ray Diffraction, third ed., Prentice Hall, Inc., 2001.
13. K. Vishista, F.D. Gnanam, Role of deflocculants on the rheological properties of boehmite sol. J. Mat. Let. (2003) 10.029 https://doi.org/10.1016/j.matlet.2003.10.029
14. R.H. Doremus, Bioceramics, J. Mater. Sci. 27 (1992) 285–297. https://doi.org/10.1007/BF00543915
15. S.M. Londoño-Restrepo, C.F. Ramirez-Gutierrez, A. del Real, E. Rubio-Rosas, M.E. Rodriguez-García, Study of bovine hydroxyapatite obtained by calcination at low heating rates and cooled in furnace air, J. Mater. Sci. 51 (2016) 4431–4441. https://doi.org/10.1007/s10853-016-9755-4
16. Y. Doi, Y. Moriwaki, T. Aoba, J. Takahashi, K. Joshin, ESR and IR studies of carbonate-containing hydroxyapatites, Calcif. Tissue Int. 34 (1982), 178–181. https://doi.org/10.1007/BF02411230
17. S.A. Manafi, B Yazdani, M.R. Rahimiopour, S.K. Sadrnezhaad, M.H. Amin, M. Razavi, Synthesis of nano-hydroxyapatite under a sonochemical/hydrothermal condition, Biomed. Mater (2008) Jun; 3(2):025002 https://doi.org/10.1088/1748-6041/3/2/025002
18. I. Rehman, W. Bonfield, Characterization of hydroxyapatite and carbonated hydroxyapatite by photo acoustic FTIR spectroscopy, J. Mater. Sci. Mater. Med. (1997) 8:1-4. doi: 10.1023/A:1018570213546
19. S. Habelitz, L. Pascual, A. Durán, Nitrogen-containing apatite. J. Eur. Ceram. Soc. 19 (1999) 2685–2694. doi:10.1016/ S0955-2219(99)00048-5
20. M. Markovic, B.O. Fowler, M.S. Tung, Preparation and Comprehensive Characterization of a Calcium Hydroxyapatite Reference Material. J. Res. Natl. Inst. Stand. Technol. (2004) 109(6), 553–568. https://doi.org/10.6028/jres.109.042
21. M.A. Giardina, M.A. Fanovich, Synthesis of nanocrystalline hydroxyapatite from Ca(OH)2 and H3PO4 assisted by ultrasonic irradiation, Ceram. Int. 36 (2010) 1961–1969. https://doi.org/10.1016/j.ceramint.2010.05.008
22. R.-X. Sun, Y. Lv, Y.-R. Niu, X.-H. Zhao, D.-S. Cao, J. Tang, X.-C. Sun, K.-Z. Chen, Physicochemical and biological properties of bovine-derived porous

hydroxyapatite/collagen composite and its hydroxyapatite powders, Ceram. Int. 43 (2017) 16792–16798. https://www.x-mol.com/paperRedirect/373320

23. N.A.M. Barakat, M.S. Khil, A.M. Omran, F.A. Sheikh, H.Y. Kim, Extraction of pure natural hydroxyapatite from the bovine bones bio waste by three different methods, J. Mater. Process. Technol. 209 (2009) 3408–3415. https://doi.org/10.1016/j.jmatprotec.2008.07.040
24. E. Hosseinzadeh, M. Davarpanah, N.H. Nemati, S.A. Tavakoli, Fabrication of a hard tissue replacement using natural hydroxyapatite derived from bovine bones by thermal decomposition method, Int. J. Organ Transplant. Med. 5 (2014) 23–31.
25. M.R. Ayatollahi, M.Y. Yahya, H.A. Shirazi, S.A. Hassan, Mechanical and tribological properties of hydroxyapatite nanoparticles extracted from natural bovine bone and the bone cement developed by nano-sized bovine hydroxyapatite filler, Ceram. Int. 41 (2015) 10818–10827. https://doi.org/10.1016/j.ceramint.2015.05.021
26. L. Yubao, C.P. Klein, X Zhang, K. de Groot, Relationship between the colour change of hydroxyapatite and the trace element manganese, Biomaterials 14 (1993) 969–972. https://doi.org/10.1016/0142-9612(93)90187-7
27. E. Kusrini, M. Sontang, Characterization of x-ray diffraction and electron spin resonance: Effects of sintering time and temperature on bovine hydroxyapatite, Radiat. Phys. Chem. 81 (2012) 118–12. https://doi.org/10.1016/j.radphyschem.2011.10.006
28. C. Rey, M. Freche, M. Heughebaert, J.C. Heughebaert, J.L. Lacout, A. Lebugle, J. Szilagyi, M. Vignoles, Apatite chemistry on biomaterial preparation, shaping and biological behaviour, in W. Bonfield, G.W. Hastings, K.E. Tanner (eds.) Bioceramics, vol.4, Butterworth-Heinemann Ldt., London, 1991, pp.57–64
29. Y. Sawada, M. Suzuki, Thermal change of SnI2 thin films. Part 4. TG-DTA and DSC, Thermochim. Acta. 254 (1995) 261–266. https://doi.org/10.1016/0040-6031(94)02089-7
30. M. Yetmez, Z.E. Erkmen, C. Kalkandelen, A. Ficai, F.N. Oktar, Sintering effects of mullite-doping on mechanical properties of bovine hydroxyapatite, Mater. Sci. Eng. C 77 (2017) 470–475. https://doi.org/10.1016/j.msec.2017.03.290
31. JCPDS Card File No. 9-432 (Hydroxyapatite), Joint Committee on Powder Diffraction Standards. Swathmore, PA, 1996.
32. S. Joschek, B. Nies, R. Krotz, A. Göferich, Chemical and physicochemical characterization of porous hydroxyapatite ceramics made of natural bone. Biomaterials 21 (2000) 1645–1658. https://doi.org/10.1016/s0142-9612(00)00036-3

33. C.Y. Ooi, M. Hamdi, S. Ramesh, Properties of hydroxyapatite produced by annealing of bovine bone. Ceramics Int. 33 (2007) 1171–1177. https://doi.org/10.1016/j.ceramint.2006.04.001
34. M. Jevtić, M. Mitrić, S. Škapin, B. Jančar, N. Ignjatović, and D. Uskoković, Crystal Structure of Hydroxyapatite Nanorods Synthesized by Sonochemical Homogeneous Precipitation, Cryst. Growth Des. 8, 7 (2008) 2217–2222. https://doi.org/10.1021/cg7007304

Fig. 1. (A) Pre-treatment with thermochemical action. (B) Bone cubes after calcination. (C) Gyratory mill. (D) Vibratory mill.

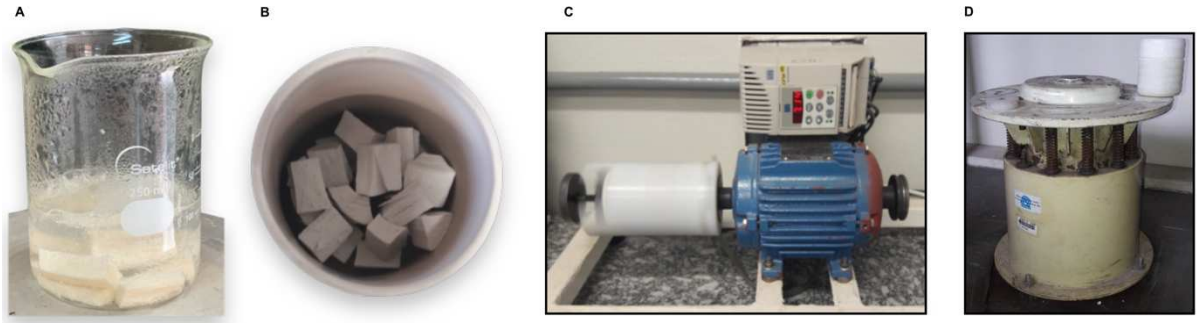

Fig. 2. FT-IR spectrum and the amplification of bands 1300 – 1500 cm^{-1} of HA precursor and after the nanoparticulation methods.

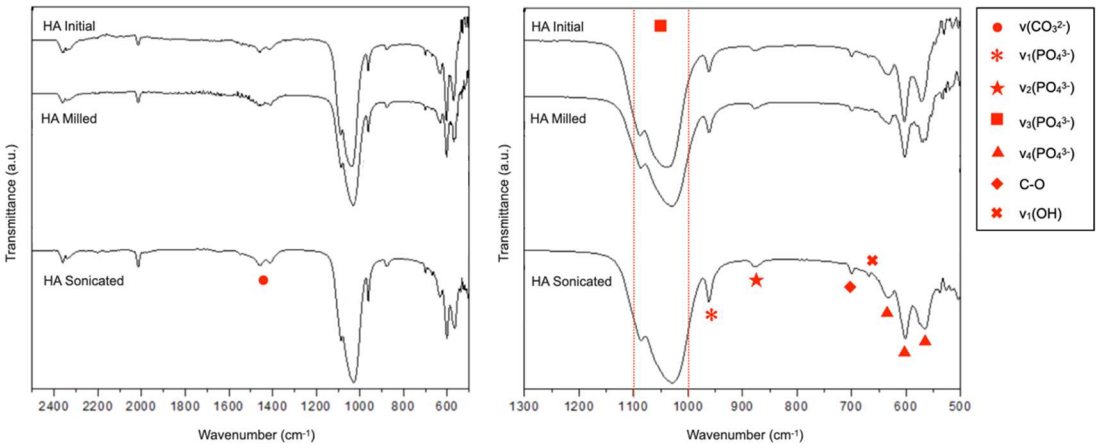

Fig. 3. The comparative XDR patterns and the amplification at 2θ 30 – 40° of HA precursor and after the nanoparticulation methods.

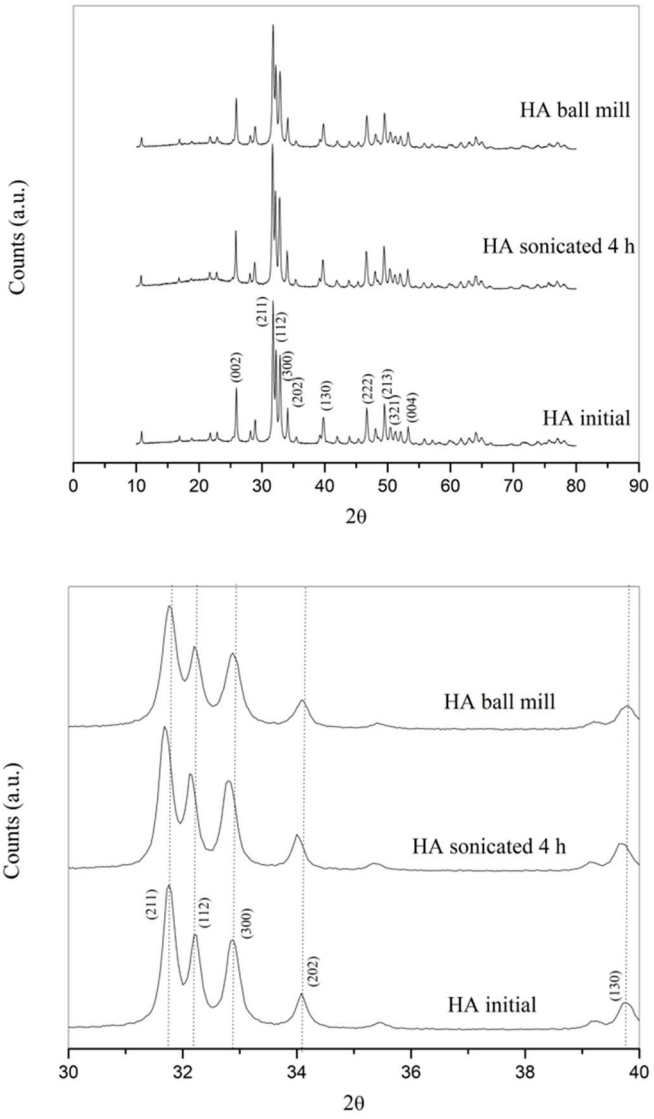

Fig. 4. Chemical characteristics for the three samples obtained by EDX.

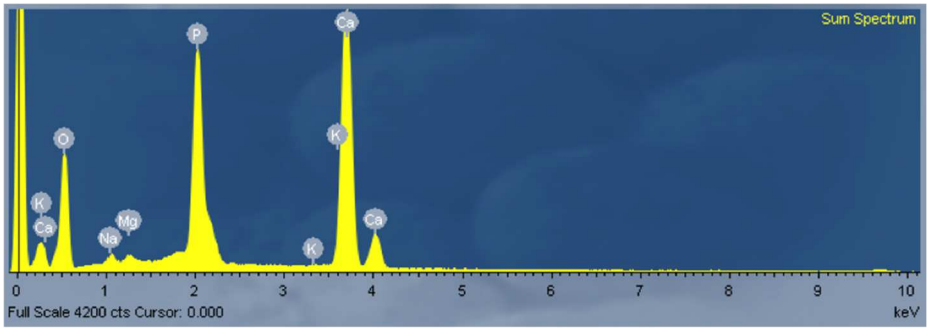

Fig. 5a. TEM micrograph of the initial HA. In detail electron diffraction shows that this is a polycrystalline sample.

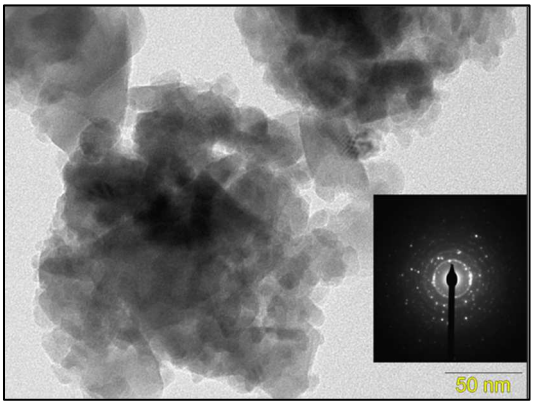

Fig. 5b. TEM micrograph of the HA sonicated sample. In detail electron diffraction shows that this is a polycrystalline sample.

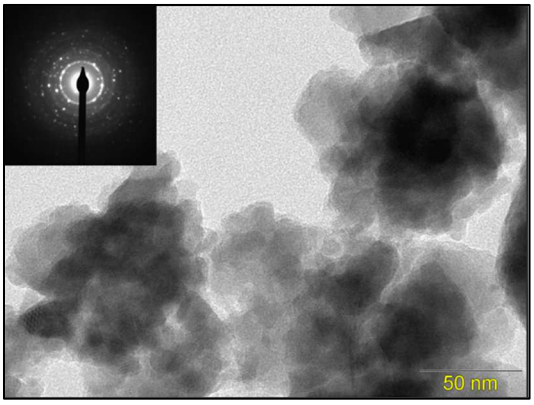

Fig. 5c. TEM micrograph of the HA milled sample. In detail electron diffraction shows that this is a polycrystalline sample.

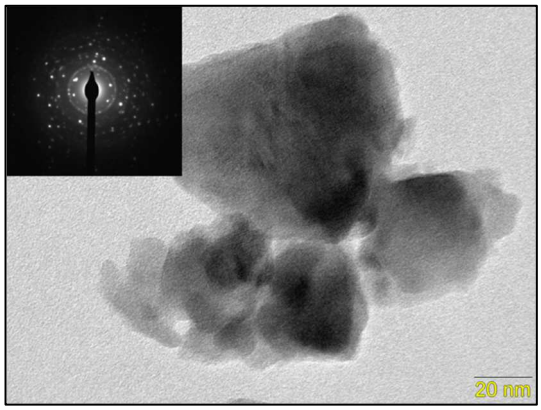

Fig. 6. TEM micrograph of initial (A), sonochemical (B) and ball mill (C) HA samples.

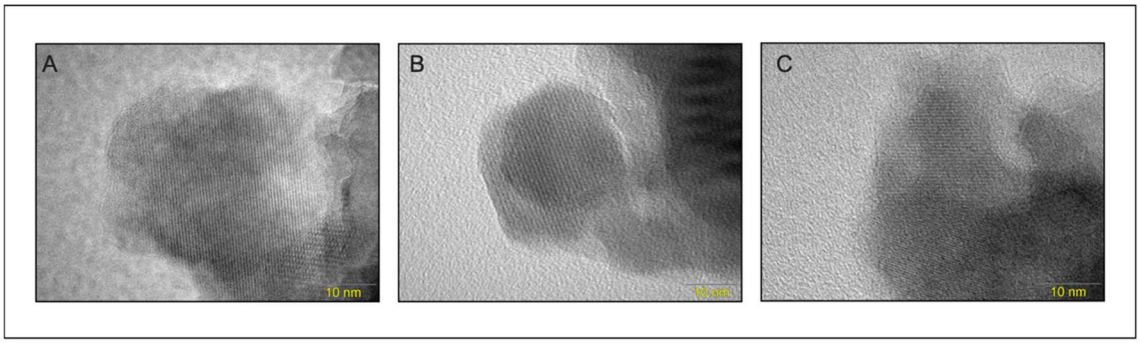

Fig. 7. TEM images allowed the construction of the distribution of number of particles histograms as a function of particle diameter for the samples sonicated and milled.

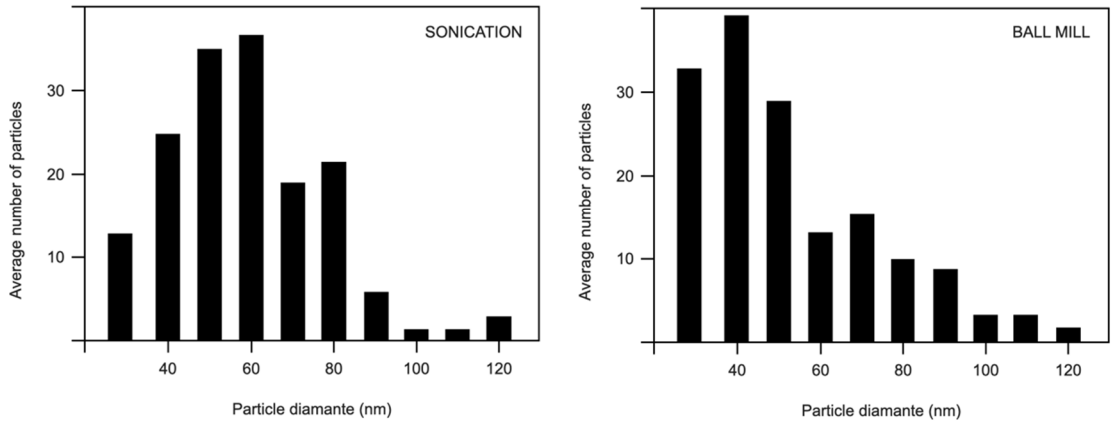

2.2 ARTICLE 2

Synthesis and characterization of an experimental silica-based composite ceramic added with nano-sized bovine hydroxyapatite

This article was written according to the Ceramics International periodic.

B. M. Ferrairo[1]; L. J. A. Silva[1]; V. Mosquim[2]; L. A. Pires[2]; D. S. S. Padovini[3]; A. G. Magdalena[3]; C. A. Fortulan[4]; P. N. Lisboa-Filho[5]; A. F. S. Borges[1,2]*; J. H. Rubo[1].

[1] Department of Prosthodontics and Periodontics, Bauru School of Dentistry, University of São Paulo, Bauru, SP, Brazil.

[2] Department of Operative Dentistry, Endodontics and Dental Materials, Bauru School of Dentistry, University of São Paulo, Bauru, SP, Brazil.

[3] Department of Chemistry, UNESP - School of Science, São Paulo State University, Bauru, SP, Brazil.

[4] Department of Mechanical Engineering, São Carlos School of Engineering, University of São Paulo, São Carlos - SP, Brazil.

[5] Department of Physics, School of Sciences, São Paulo State University, Bauru - SP, Brazil.

*Corresponding author: Ana Flávia Sanches Borges, Alameda Dr. Octávio Pinheiro Brisolla, 9-75, Vila Universitária, ZIP CODE: 17012-901. Bauru, São Paulo, Brazil. Telephone: +55 014 3235-8000. e-mail: afborges@fob.usp.br

ABSTRACT

This study aimed to produce an experimental dense SiO_2/HA composite ceramic via uniaxial/isostatic compression that was physicochemical and microstructurally characterized varying the sintering temperature and the addition of PVB. Ball mill technique was used to mixture fumed silica and nano-HA from bovine bone source. Groups are divided into 3, 5 and 10% of HA addition, 1.2 and 2.4 wt.% of PVB, and 1100, 1200 and 1300 °C for maximum temperatures to firing plateau (4h). Characterization was performed by Scanning Electron Microscopy (SEM), Energy Dispersive X-ray Spectroscopy (EDX), X-ray Diffraction (XDR) and Fourier Transform Infrared (FTIR). Considering the microstructural evolution, the temperature of 1200 °C presented potentialized chemical bonds without the degradation of HA at XDR profile. As the temperature increases the HA is degraded, losing the calcium-phosphate bands and consequently the CO_2 band becomes more prominent at FTIR spectra. The concentration of PVB showed no chemical changes in the experimental composite ceramic. SEM images suggests that 2.4 wt.% of PVB result in optimized compaction and a lower incidence of cracks and pores, which should be investigated using additional supporting methods. It is noteworthy that additional methodologies are necessary for a complete scan of composition possibilities. Nevertheless, this study suggests that the SH composite ceramic with 5% of HA with 2.4 wt.% of PVB, sintered at 1200 °C, exhibit potentially superior properties to biomaterial applications.

Key words: Ceramic material; Nanoparticles; Nanostructured materials; Silica; Hydroxyapatite; composite particles.

1. Introduction

Studies about synthesis of bioceramics have drag attention due to its wide applicability in orthopedics and dentistry reconstructing and repairing musculoskeletal system. Termed bioceramics may be bioinert (zirconia, alumina), resorbable (tricalcium phosphate), porous for tissue ingrowth (hydroxyapatite-coated metals, alumina), or bioactive (hydroxyapatite, glass-ceramic, bioactive glasses) [1]. Silicon is often present in bioceramics composition because it is an important micronutrient for bone and connective tissue health [2,3], participating in the early stages of bone mineralization by directly stimulating and upregulating osteoblasts proliferation [4-6] and gene expression [7,8]. High concentrations ($\geq$ 30-50 wt.% of SiO_2) have been investigated that perform surface reactions on initial cellular and ionic process, allowing the crystallization of apatite crystals, collagen formation and cell adhesion [9-11].

Hydroxyapatite [$Ca_{10}(PO_4)_6(OH)_2$] (HA) is thermodynamically stable in its crystalline state in body fluid and has a special chemical composition that is morphologically and structurally similar to the mineral portion of human's bone [12]. HA can be chemically synthesized by several methods extensively studied, because of the possible of formation of toxic intermediary products during the process or extracted from biological sources or wastes such as mammalian bone [12,13]. Bovine bone has the benefit of being easily available and for being an inexpensive source associated with Ca/P ratio, particles shapes and crystalline phases favorable to use as bioactive material [13]. Bioactivity and osteoconductive properties coexist with mechanical properties insufficient for monolithic load-bearing use [14].

The association between Si-HA was proposed two decades ago and has been promising ever since [14]. Significant bone formation [15,16], enhanced bone attachment [17,18] and long-term Si delivery system [19] are promising characteristics of this association in different arrangements, e.g., granules [20], microspheres [21], plasma-sprayed coatings [9], scaffolds [22], porous [23] and dense bioceramics [24]. Although the association Si-HA has been much discussed, there is a gap in the literature regarding the densified conformation with silica matrix and HA acting as its additive. Sintering temperature, timing and atmosphere, starting powder grain size and shape, pressure, composition and preparation methodologies are some factors that influence on dense ceramics preparation [25-27]. Choices such as the use of nanocrystalline starting powders and compaction by uniaxial/isostatic pressing were made in order to produce an optimized sintering ability and low-cost material production [28,29].

Considering the obstacles at reaching proper composition, particle size, synthesis process, microstructural and physicochemical properties, idealizing an experimental material

combining SiO_2 and HA (SH composite ceramic) would help the biomaterial science. SH could present a high bioactivity through the release of dissolution ions such as Si, Ca and P, which may also affect vascularization, gene expression in osteogenic cell, and consequently improve bone formation [30-34]. Therefore, since high silicon material associated with HA has been produced by different processing methods and achieved interesting results, the aim of this study was to produce a new glass ceramic containing SiO_2/HA via uniaxial/isostatic powder compression and structurally and chemically characterize this material, varying the sintering temperatures and concentration of binder.

2. Experimental procedures

2.1. Nano-sized hydroxyapatite

HA was obtained from bovine femurs. The femoral body portion was cut into pieces of approximately 1 cm^3 and were embedded in hydrogen peroxide (H_2O_2) as a 30 %, 100 volume aqueous solution, and heated to 100 °C [35]. After removing the apparent organic matter, the samples were calcined with a heating curve up to 900 ºC (5 °C / minute) and a two-hour plateau [36,37] to finalize the pre-treatment step. After gradual cooling, they were ground manually, and the powder sieved (# 200 mesh ≤ 75 μm).

The nanoparticulation process was performed with the aid of a ball mill. A 300 cm^3 capacity polyethylene jug was filled with 40 vol% (500 g / 100 ml) of griding elements (spheres of 3Y zirconia Ø 10 mm), 30 vol% of HA, 70 vol% of isopropyl alcohol (C_3H_8O) and 0.05 wt.% of para-aminobenzoic acid ($H_2NC_6H_4CO_2H$, PABA), and placed for 96 hours in a vibrating ball mill. After this period, 1.2% by weight of polyvinyl butyral ($(C_8H_{14}O_2)_n$, PVB) was added over the weight of HA, which was mixed and homogenized in a rotary ball mill for 2 hours. The content was dried with a hot air blower at approximately 80 ° C and granulated in stainless steel sieves (# 200 mesh ≤ 75 μm).

2.2. Synthesis of experimental material

For the matrix of the experimental material, fumed silica (SiO_2, Sigma-Aldrich) was used, with particle size of 0.007 μm, surface area of 395 ± 25 m^2/gram and density of 2.3 lb./cu. ft. The study variables were (1) the percentage of HA addition, (2) the temperature of the sintering plateau, and (3) the concentration of PVB (Table 1).

Table 1

Groups distribution according to the study variables

HA %	Sintering temp.	PVB wt%
3 %	1100 °C	1.2 wt%
5 %	1200 °C	2.4 wt%
10 %	1300 °C	

The mixing of the experimental material was mechanically carried out in a ball mill. Since the molecular weight of amorphous SiO_2 is 2.2 g/cm^3 and of HA is 3.156 g/cm^3, the jug was filled with 40 vol% (500 g / 100 ml) of griding elements (spheres of 3Y zirconia Ø 10 mm), 30 vol.% of SiO_2 + HA, 70 vol.% of isopropyl alcohol and 0.05 wt.% of PABA, and was placed for 2 hours in a rotatory ball mill. After this period, 1.2% or 2.4 wt.% of PVB, previously diluted in isopropyl alcohol, was added to the jug and mixed and homogenized in a rotary ball mill for 10 minutes (Table 2).

Table 2

Solid content used in proportion to the synthesis of the experimental material

	SiO_2	HA	C_3H_8O	PABA	PVB
SiO_2 + 3% HA	53.35 g	2.36 g	56.50 g	0.28 g	2.52 g / 5.04 g
SiO_2 + 5% HA	52.25 g	3.94 g	56.50 g	0.28 g	2.52 g / 5.04 g
SiO_2 + 10% HA	49.50 g	7.89 g	56.50 g	0.28 g	2.52 g / 5.04 g

The content was oven dried at approximately 80 °C and granulated in stainless steel sieves (# 200 mesh ≤ 75 μm). The powder was proportioned and pressed in a uniaxial press (100 MPa / 30 sec), with the aid of matrix that was lubricated with a thin layer of oleic acid ($C_{18}H_{34}O_2$). Once compacted, the specimens were vacuum packed and received the second compactation in an isostatic press (200 MPa / 1 min).

The silica-hydroxyapatite composite ceramic samples were sintered in atmosphere air by a chamber-type oven (Lindberg Blue / M). Sintering scheme is describe in Figure 1.

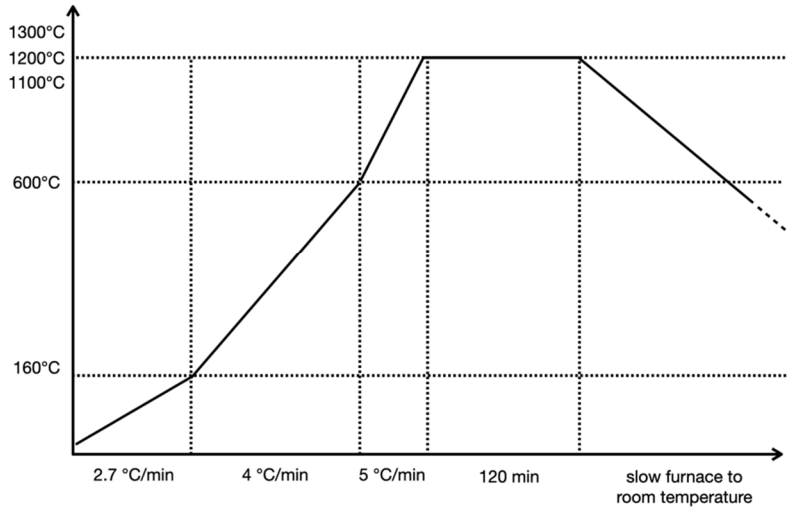

Fig. 1. Sintering scheme in atmosphere air by a chamber-type oven (Lindberg Blue / M). Plateau temperatures varied according to the groups studied (1100, 1200 or 1300 °C).

2.3. Characterization methods

Four different investigative techniques were used to analyze morphologically, chemically and structurally the samples: scanning electron microscopy (SEM), energy dispersive x-ray spectroscopy (EDX), x-ray diffraction (XDR) and Fourier transform infrared (FTIR). They were performed on the starting powders, the blend of powders before sintering (initial characterization) and the pellets after sintering (final characterization), aiming to compare them and observe the changes caused by sintering and variations in the concentration of HA and PVB.

2.3.1. SEM/EDX

The samples were coated with gold at ≅ 10 nm thickness and were investigated using an XL30 FEG, an ultra-vacuum system with the base pressure of 1×10^{-5} Pa and an acceleration voltage of 20 kV. Images were taken using a JEOL-JSM 56000LV microscope (Tokyo-Japan), equipped with an X-ray detector (Voyager, Noran Instruments) which allowed the chemical elements analysis under vacuum in backscattered electron mode.

2.3.2. .XDR

Samples were characterized by X-ray diffraction on a Rigaku Miniflex600 X-ray diffractometer using CuKα radiation source (λ = 1.54056 Å) with rotatory anode operation at 40 KV and 150 mA.

The amorphous characteristic of the fumed silica powder and the crystalline phases of HA were identified and validated by XDR. In order to propose standards and evaluate the profiles, the Joint Committee on Powder Diffraction and Standards (JCPDS) was used. Some of the cards selected was: # 29-0085 for amorphous SiO_2, # 024-0033 for HA, # 009-0080 for $CaHPO_4$, # 001-1160 for CaO, and # 001-0941 for $Ca_3(PO_4)_2$.

2.3.3. FTIR

Spectra were recorded using KBr pellets (FTIR-Vertex 70, Bruker), in the transmittance mode with the range of 500-2500 cm-1, in order to investigate the functional groups of resultant powders.

3. Results and discussion

3.1. Silica and HA powder characterization

The use of fumed silica for the experimental ceramics was motivated by the submicron-size of its spheres. The smaller the particles, the larger the estimated surface area. This correlation results in a larger area available for interaction with nano-HA and the unique particle flocs promote a dispersion to mechanical stress [38]. The alcoholic medium was attempted to not exceed the threshold concentration (Pg) because the viscous liquid characteristic is beneficial for ball-mill method making the dilute dispersion flowable when perturbed by mechanical action [39]. Associating fumed silica and polar organic solvents tends to form low viscosities medium and networks of overlapping agglomerates and clusters [38,40]. Hydrogen bonding between silanol groups on different particle surfaces are caused by the attractive interactions between particle aggregation and network formation [40,41].

Bovine bone is a well-studied natural source of HA with predictable and reliable characteristics [13]. Due to the structural and morphological similarity with the human bone, the cortical portion of the femur was chosen for the study [42]. The pre-treatment step completely removed the collagen, lipids and non-collagenous organic proteins from the bone matrices [43], remaining only the mineral phase (HA).

XDR analysis of the silica fumed and HA as shown in Figure 2 exhibited peaks within the $2\boldsymbol{\theta}$ range from 10° to 80° that corresponds to stoichiometric of the amorphous structure of SiO2 (JCPDS no. 29-0085) and HA (JCPDS no. 9-432). No phase decomposition (CaO, TTCP, a-TCP and b-TCP) was found and it can be observed the high crystallinity and single phase on

HA spectra of starting powder. This finding highlight that the sintering treatment produced pure HA.

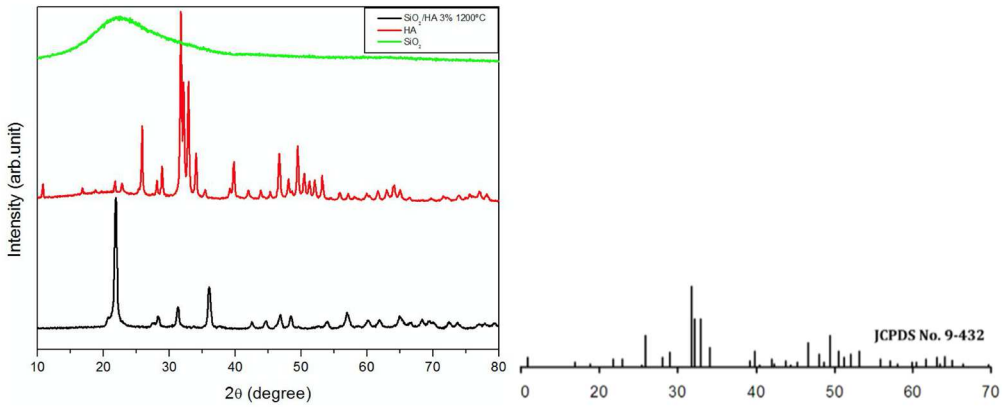

Fig. 2. XDR pattern of SiO_2, HA and SiO_2 + 3% HA (1200 °C) group. Correspond to the characteristic peak of SiO_2 (JCPDS no. 29-0085) and of HA (JCPDS no. 9-432).

The IR spectrum of starting powders coincide with those described in the literature. Silica fumed presents the vibration of Si-O-Si [44] and Si-OH bonds [45] while the inorganic phase of HA is composed mainly of Ca and P with some minor components (Na, Mg, O, and C) [46]. Spectrum of HA shows the presence of major inorganic species, phosphate (from the mineral HA), carbonate (from carbonate substitution for hydroxyl and phosphate groups in HA), and organic components such as amide functional groups I–III from the protein constituents of bone (mainly type I collagen) [47].

3.2. SH (silica-hydroxyapatite) composite ceramic conception

3, 5 and 10 % of nano-HA were selected (Table 1) based on previous studies with silica-based ceramics that receive addition of crystalline material, such as ZrO_2 [29,48], and studies that associate SiO_2 and HA [49,50]. The homogeneously distribution of HA nanoparticles enhance the mechanical and tribological properties acting as load carries [36]. Increasing the proportion of HA results in greater challenge for homogeneous distribution within the bulk, which may result in aggregated particles and formation of mechanical deficiency regions. However, a higher concentration can provide greater bioactivity to the material [51].

In order to favor the compacting and pressing of specimens, PVB was used as a binder in this study. An amorphous thermoplastic that presents an excellent flexibility, fil-forming and adhesion, PVB could functioned as a cross-linked according to the number of residuals OH groups in the material [52]. The flakes conformation of fumed silica has a great oxygen coating

in ambient conditions and, although the use of binders can provide the formation of porosities in the material [53,54], its absence could make the manipulation of the specimens unfeasible after pressing [54,29].

Sintered SH composite ceramic results

The association between the uniaxial and isostatic compaction technique [53] with the mechanical method of the ball mill [29] has been successfully used in the synthesis of ceramics with high density and mechanical resistance. These steps favored the bulk homogenization and the specimen conformation, preparing them for sintering.

In this study, the plateau temperature was varied aiming to observe the reflects on physicochemical characteristics of SH composite ceramic and predict the optimal sintering scheme. Although the fusion temperature of silica is 1710 °C, further collisions result in some irreversible mechanical entanglement or agglomeration from 800 °C [55] and around 1250 – 1300 °C the compaction can occur [56]. Once the decomposition of HA initiate at 1250 – 1300 °C and reflects in grain boundaries and deterioration of mechanical properties of ceramics [57-59], the elected temperatures were 1100, 1200 and 1300 °C to sinter the green-body specimens.

A low sintering scheme was used in order to stablish a graduation of temperature favoring, i.e., the effective burn out of binder at 600 – 700 °C [49], reducing the imprisonment of CO_2 on composite ceramic body. Band at 2300 cm-1 could indicate these CO_2 imprisonment [60] inside the bulk of the material on FTIR analysis (Figure 3).

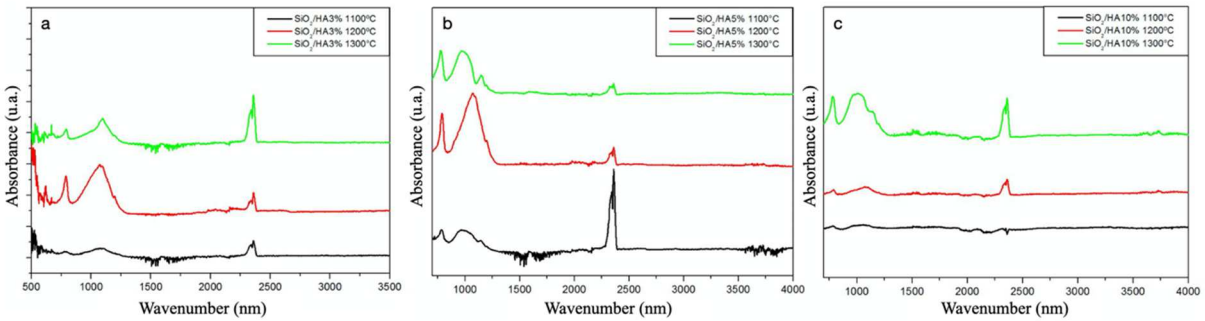

Fig. 3. FTIR pattern of SH composite ceramic in different concentration of nano-HA, 3 (a) 5 (b) and 10 % (c), sintered at 1100, 1200 and 1300 °C.

For concentrations of 3 and 10% HA, according to the sintering temperature, the bands of CO_2 became more prominent, while for the concentration of 5% this relationship was reversed. Figure 4 presents the three concentration groups sintered at 1200 °C and demonstrates

controlled peaks of CO_2. Spectra exhibits vibrational modes that can be attributed to bound (3700 – 2600 cm^{-1}) and free (3571 cm^{-1}) hydroxyl stretch modes, the carbonate asymmetric stretch (1638 cm^{-1}) and out of bending mode (875 cm^{-1}), and the phosphate asymmetric stretch (1088/1047 cm^{-1}), and v_4 O-P-O in plane bending modes at 637 cm^{-1} [61-64]. Vibrational modes from silanol (Si-OH) stretch region stretch region (3700–2500 cm^{-1}), Si–O stretch (1100 and 962 cm^{-1}), Si-OH deformation vibration (1020 cm^{-1}) and bonded silanol groups 3400-3200 cm^{-1}, and the characteristic Si–O–Si stretch near 480 cm^{-1} did not appear in spectra, only in 1130-1000 cm^{-1} [65].

It is interesting to note that HA and SiO_2 share a number of similarly spaced vibrational modes near 3700– 2500 cm^{-1} (hydroxyl stretch), 1635–1640 cm^{-1} (carbonate), 1089–1095 cm^{-1} (Si–O/P–O stretch), 958–962 cm^{-1} (Si–O/P–O symmetric stretch), and 477–483 cm^{-1} (Si–O–Si stretch/P–O out of plane bending) that are not represented on Figures 3 and 4. This may be attributed to similarities in vibrational characteristics between the SiO_4^{4-} and PO_4^{3-} tetrahedral molecular units that are incorporated into the structures of SiO_2 and HA [64].

The intensities of the weak surface P-OH vibrational mode at 3682 cm^{-1} [61], the free hydroxyl stretch at 3571 cm^{-1}, the n_3 phosphate peaks at 2100, 1088, and 1047 cm^{-1}. In addition, the carbonate n_2 mode at 875 cm^{-1} and the n_3 carbonate modes at 1638, 1455, and 1421 cm^{-1} decrease in intensity with increasing silica-coating amount.

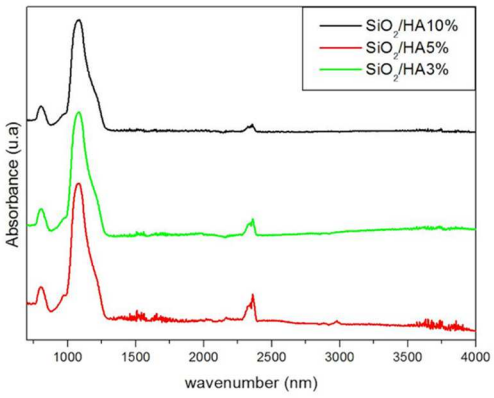

Fig. 4. FTIR pattern of SH composite ceramic sintered at 1200 °C.

The specimens after sintering were analyzed via XDR (Figure 5), an interesting method to identify the phases in every group of sintering process. The intensity of the major peak of the sintered SH at 1200 °C has a vivid increase in comparison with XDR analysis of sample 1100 and 1300 °C, which indicates the increase of powder's crystallinity. The temperature of 1100 °C presented an attempt of binding with substantial increase in FWHM. At 1200°C the peaks

were evidenced and at 1300 °C the degradation already prevented its increase, the HA peaks start to disappear and the formation of $Ca(OH)_2$ peaks are promoted. The intensity of the characteristic peaks for b-tricalcium phosphate (***β***-TCP), located at 2***θ*** angles of 27.75, 31.65, 45.55, and 48.00° are more prominent at 1200 °C group, temperature that would cause the HA decomposition into *α*-TCP {Ca3(PO4)2}, ***β***-TCP {Ca3(P2O8)} and calcium oxide (CaO) [46].

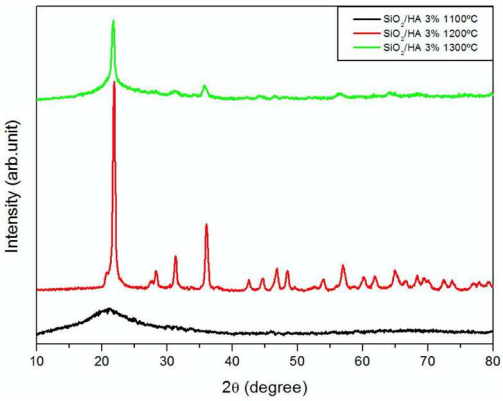

Fig. 5. XDR pattern for SH composite ceramic with 3% of HA sintered at 1100, 1200 and 1300 °C.

The chemical characterization of starting powders (SiO_2, HA and SH composite ceramic blends) and after sintering was conducted using SEM/EDX. The EDX analysis detected silicon (Si) and oxygen (O), in 46.08 wt.% and 53.92 wt.%, respectively. To HA sample, EDX detected calcium (Ca) 27.38 wt.%, phosphate (P) 12.92 wt.%, carbon (C) 8.69 wt.%, sodium (Na) 0.72 wt.%, magnesium (Mg) 0.48 wt.%, and oxygen (O) 38.94 wt.%.

Aiming to characterize the effects of the sintering temperature variation, SEM was conducted on bulk area. Figure 6 illustrate the SH composite ceramic with 10% of HA sintered at 1100 (a, b, c), 1200 (d, e, f) and 1300 °C (g, h, i). Insufficient densification of the sample can be observed with pores and cracks in the material, functioning as potential areas to catastrophic failure during eventual mechanical challenge. Some pores can also originate from the evaporation of the PVB. At 1100 °C the flaking aspect of the agglomerated fumed silica, although compacted, continues to be observed at higher magnifications (Figure 1b, c), in agreement with the findings of physical-chemical analysis. At temperatures of 1200 °C and 1300 °C the matrix is more homogeneous, with union of particles. However, the pores of the highest temperature appear to be of higher volume.

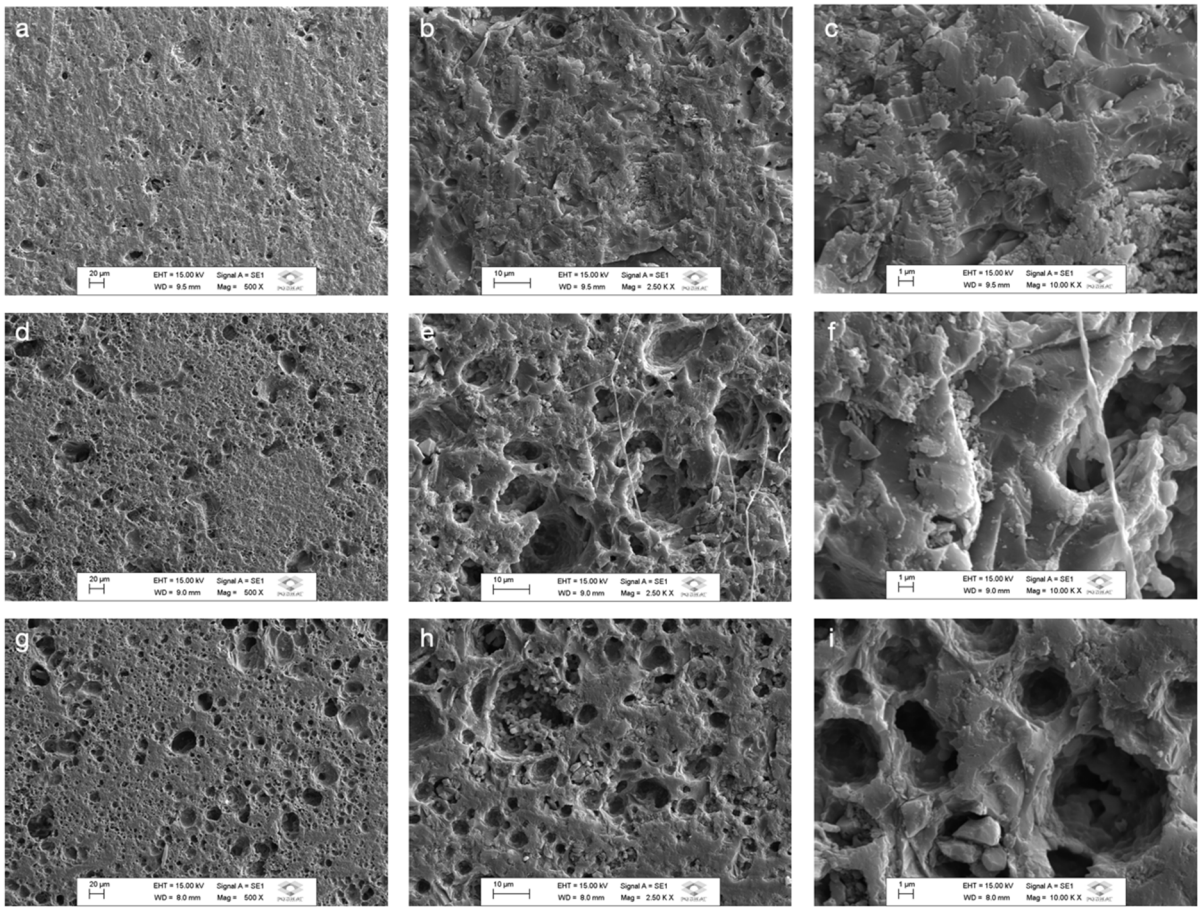

Fig. 6. SEM images of SH composite ceramic with 10% of HA sintered at 1100 (a, b, c), 1200 (d, e, f) and 1300 °C (g, h, i).

The starting powders of starting powder of SiO_2 and HA can be seen in Figure a and b, respectively. Bends before and after sintering at 1200 °C are presented at Figure 7 and help to compare the structural change that has occurred. The greater the addition of HA, the more evident the filaments within the ceramic bulk. They are most noticeably maintained at 1200 °C (Figure 6 e, f and Figure 7 h) and according to EDX their composition is mostly magnesium. It was observed on the concentrations studied, but other concentrations could be investigated and a range of sintering temperature between 1200 and 1300 °C is valid to be exploited.

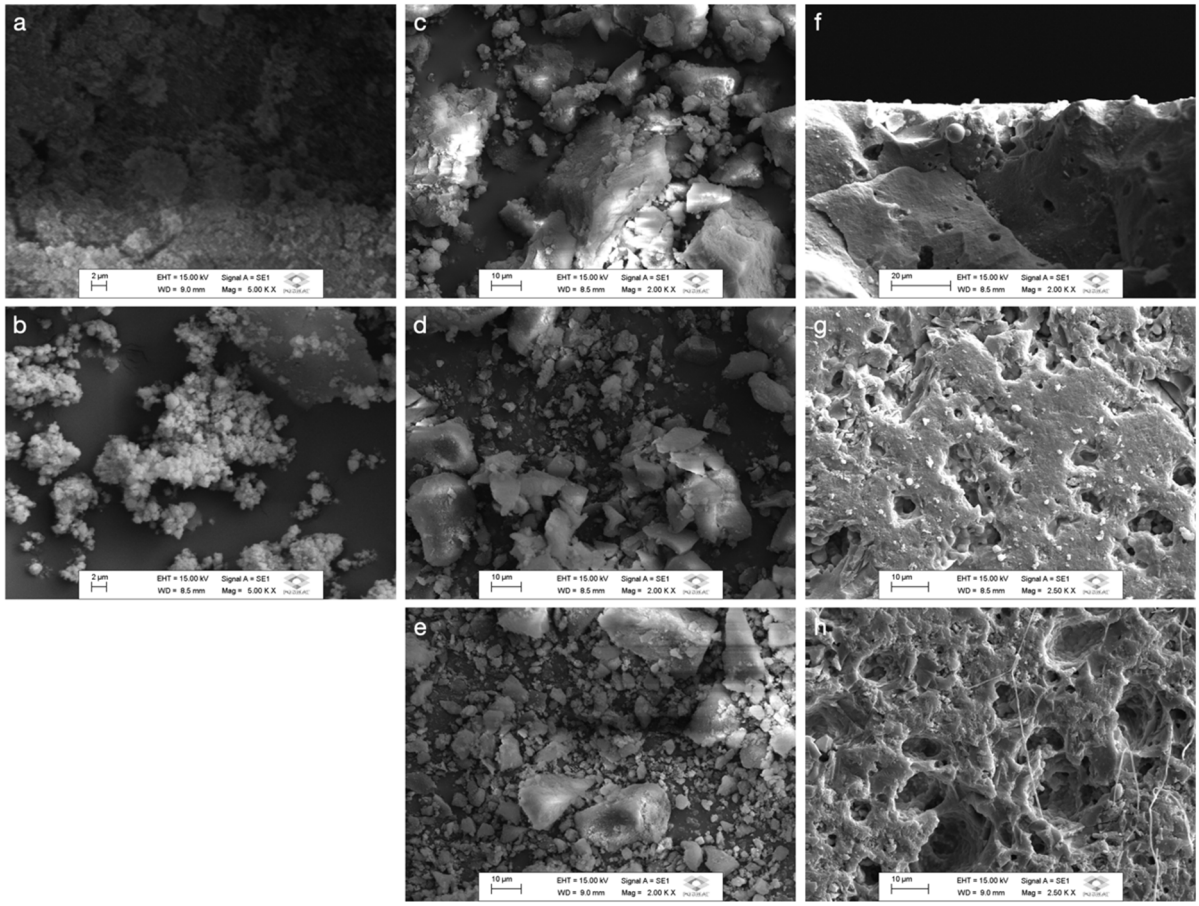

Fig. 7. SEM images of starting powder of SiO_2 (a), HA (b), SH composite ceramic with 3% of HA (c), 5% of HA (d) and 10% of HA (e). After sintering at 1200 °C the SH composite ceramic with 3% of HA (f), 5% of HA (g) and 10% of HA (h).

3.4. PVB concentration results

The use of a binder is essential because of the hard and limited plastic deformation capability of a ceramic powder at room temperature [66]. Lubricant, in this case the oleic acid, is used in small quantity and should not infer on adhesive forces between particles. To plastically deform in between particles and transmit sufficient strength to the green compact, PVB helped to maintaining the integrity during pre-sintering handling [54]. Although, the use of organic binders requests the effective remotion in a long heating time, releasing gases that may lead the deformation of the green compact or the initiation of cracks.

PVB is usually used in necessity of a strong binding, with the ability of adhesion in different surfaces and characteristics such as toughness, flexibility and optical clarity [67]. The heat-resistance of PVB is deficient due to their low glass-transition temperature (T_g) [68]; therefore, the binder performs its stabilization function and as the ceramic is sintered it will be

eliminated at 600 – 700 °C [49]. Containing a hydroxyl group via polyvinyl alcohol (PVA) that dominates the adsorption on SiO_2 by hydrogen bonding, interaction already described between PVB and yttria-stabilized zirconia (YSZ) [69]. The high number of hydroxyl groups possibility a more effective adsorption of PVB on the ceramic particles.

Figure 8 shows SEM images of SH composite ceramic with different concentration of HA, sintered at 1200 °C, produced with 1.2% or 2.4 wt.% of PVB. EDX maintained the dispersion previously described and the groups with the highest concentration of PVB showed a slight increase in carbon levels. In lower magnifying cracks can be seen in SH composite ceramic with 3% and 10% of HA, being more frequent in groups with less HA addition (Figure 8a, c). The group of 10 % of HA and 2.4 wt.% of PVB did not present them anymore. All groups have apparent pores, which indicates inefficiency in the compaction of green body samples. Qualitatively, it can be observed that groups with 2.4 wt.% of PVB have fewer pores, which suggests a more effective compaction.

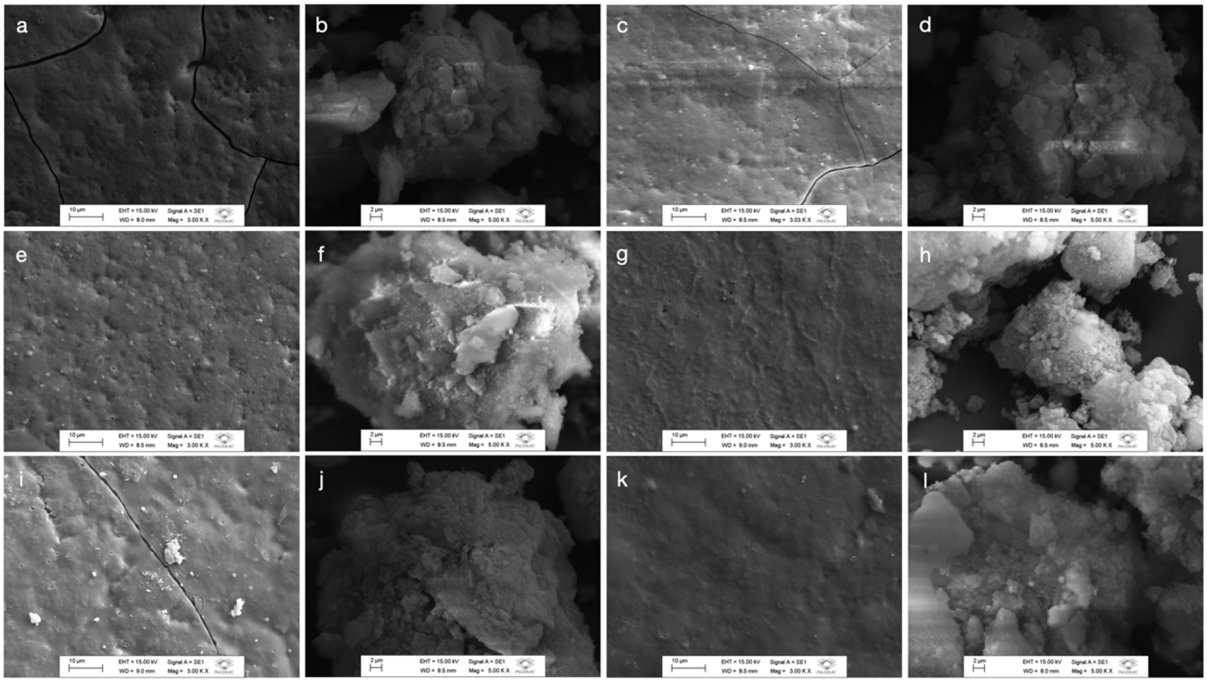

Fig. 8. SEM images of SH composite ceramic with 3% of HA 1.2% (a, b) and 2.4 wt.% of PVB (c, d), 5% of HA 1.2% (e, f) and 2.4 wt.% of PVB (g, h), and 10% of HA 1.2% (i, j) and 2.4 wt.% of PVB (k, l), sintered at 1200 °C.

XDR patterns for all samples studied are grouped at Figure 9. SiO_2 is the predominant peak at 22° in addition to low and mean intensity peaks corresponding to $Ca_5(PO_4)_3(OH)$ and β-TCP (30 – 35°) [58], revealing that these phases tend to be maintained independent of PVB

wt.% variation once de sintering temperature is the same (1200 °C). There was a maintenance of the general intensity of the spectrum, not varying significantly according to the change in concentration of the PVB, which suggests complete burn out. The volume of pores within the sample, with eventual $Ca(OH)_2$ imprisonment.

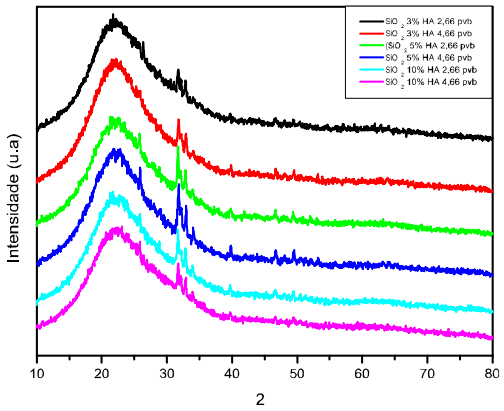

Fig. 9. XDR pattern of SH composite ceramic with different concentration of HA, varying in 1.2% and 2.4 wt.% of PVB, sintered at 1200 °C.

Analysis of FTIR spectra for PVB variation shows that all samples have typical absorption bands of SiO_4^{4-} at 1100, 1277, and 825 cm^{-1}. Indicating the crystalline HA, PO_4^{3-} presented bands at 1050, 961, 604, and 572 cm^{-1}, OH^- at 3574, 3440, 1630, and 634 cm^{-1}, CO32- carbonate groups at 1550, 1457, 1415, 880, and 800 cm^{-1} (Figure 10). It was not possible to observe changes in the spectrum in relation to the variation of the binder, between blends of starting powders and after sintering.

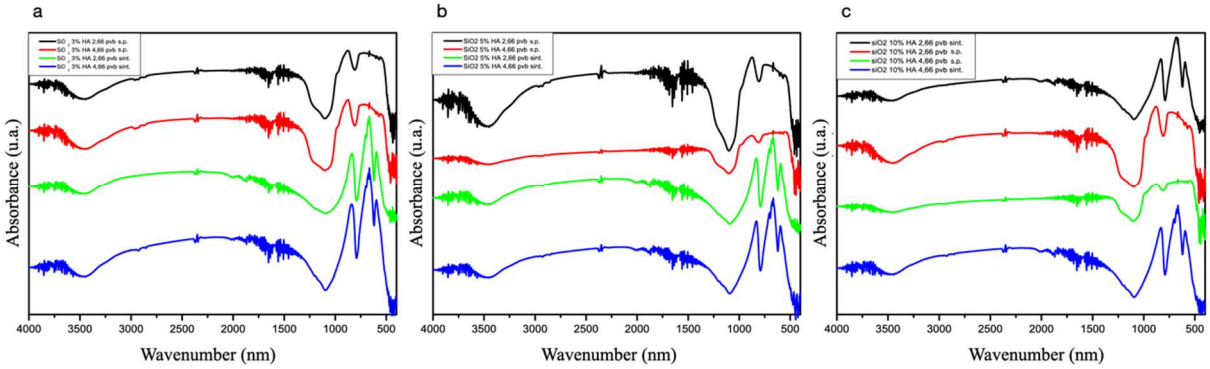

Fig. 10. FTIR pattern of SH composite ceramic. Comparison between starting powder (s.p.) and after sintering (1200 °C) varying in 1.2% and 2.4 wt.% of PVB.

According to the XDR and FTIR analysis, it can be observed that the use of presence of 1.2% or 2.4 wt.% of PVB did not influence the physicochemical characteristics of the experimental material. However, a higher concentration seems to have contributed to a more effective compaction of the green-body specimens, providing a lower incidence of cracks and apparent pores.

3.5. SH (silica-hydroxyapatite) composite ceramic results

In the present work, the nano-HA derived from bovine femurs was incorporated into a commercial fumed silica as an application of biomaterial. The study of synthesis details and characterization helped to understand the experimental material and outline future strategies to optimize it. The association between silica and HA are implement as filled cement [36] and bone substitute material [70], due to their cell proliferation ability [71], early bone ingrowth and repair [22,72,73], induction an osteogenic signal to human mesenchymal stem cells [78], and biomimetic properties [70].

As described, not only the composition but also the processing technique can be responsible to physicochemical and mechanical properties of composite ceramic. It is worth noting that a porosity between 60 – 80% stimulate the osteoconductivity and biodegradability for bone substitute [79]. The variation in sintering temperature is directly linked to the process of devitrification of the amorphous silica used. Considering that temperatures between 1200 – 1350 ºC the sintered silica powder maintained the porosity and surface area during crystallization anneal [80,81], the maximum temperature selected to the present study was 1300 ºC. The addition of HA can alter the nucleation and crystal growth temperatures of devitrification process, reflecting on mechanical properties [82]. The characterization step is essential to guide the research line and direct the best composition and microstructural pattern for the development of subsequent tests. Critical planning and analysis will save laboratory time and financial resources. Previous studies have reported that the homogeneity of bulk, which depend on powder mixer, medium and mixing procedure, has a significant influence on the properties of ceramic [37,29,83].

Therefore, more investigations are needed with SH composite ceramic in order to elucidate the physicochemical, mechanical and tribological properties deepening variations and analysis of the manufacturing routes, the matrix chemical composition, different conformation of the silica particle, and the uniformization of the HA dispersion. In this way, the positive characteristics from the SH ceramic composition such as bioactivity, biocompatibility and

osteoconductivity, which are widely studied, will provide the applicability of the experimental material by medical and dental community.

4. Conclusion

In the present work, a silica-hydroxyapatite composite ceramic was successfully produced and investigated according to physicochemical analysis. It was found that:

1- The nano-hydroxyapatite produced from bovine femurs was feasible for the composition of an experimental composite ceramic.

2- Considering the microstructural evolution, the temperature of 1200 °C presented potentialized chemical bonds without the degradation of hydroxyapatite at XDR profile.

3- The concentration of PVB showed no chemical changes in the experimental composite ceramic. SEM images suggests that 2.4 wt.% of PVB result in optimized compaction and a lower incidence of cracks and pores, which should be investigated using additional supporting methods.

4- The results suggested that the SH composite ceramic with 5% of HA with 2.4 wt.% of PVB, sintered at 1200 °C, presents potential superior properties to biomaterial.

Acknowledgment

This work was supported by the São Paulo Research Foundation (FAPESP), process number: 2018/23639-0. The authors would like to thank CAPES “Coordenação de Aperfeiçoamento de Pessoal de Nível Superior - Brasil - Finance Code 001".

REFERENCES

1. L.L. Hench Bioceramics – from concept to clinic J Am Ceram Soc, 74 (1991), pp. 1487-1510

2. Schwarz K, Milne DB. Growth-promoting effects of silicon in rats. Nature. 1972 Oct 6; 239(5371):333–4. PMID: 12635226

3. Jugdaohsingh R. Silicon and bone health. J Nutr Health Aging. 2007 Mar-Apr; 11(2):99–110. PMID:17435952

4. Carlisle, Edith M. "Silicon: a possible factor in bone calcification." Science 167.3916 (1970): 279-280.

5. Botelho CM, Brooks RA, Best SM, Lopes MA, Santos JD, Rushton N, et al. Human osteoblast response to silicon-substituted hydroxyapatite. J Biomed Mater Res A. 2006 Dec 1; 79(3):723–30. (doi: 10.1002/ jbm.a.30806) PMID: 16871624

6. Tang Q, Brooks R, Rushton N, Best S. Production and characterization of HA and SiHA coatings. Journal of Materials Science-Materials in Medicine. 2010 Jan; 21(1):173–81. (doi: 10.1007/s10856-009- 3841-y) PMID: 19672562

7. Gao, T., Aro, H.T., Yla¨nen, H. & Vuorio, E. (2001) Silica-based bioactive glasses modulate expression of bone morphogenetic protein-2 mrna in saos-2 osteoblasts in vitro. Biomaterials 22: 1475–1483.

8. Xynos, I.D., Edgar, A.J., Buttery, L.D., Hench, L.L. & Polak, J.M. (2001) Gene-expression profiling of human osteoblasts following treatment with the ionic products of bioglass 45s5 dissolution. Journal of Biomedical Material Research A 55: 151–157.

9. Patel N, Best SM, Bonfield W, Gibson IR, Hing KA, Damien E, Revell PA. A comparative study on the in vivo behavior of hydroxyapatite and silicon substituted hydroxyapatite granules. J Mater Sci Mater Med. 2002 Dec;13(12):1199-206. doi: 10.1023/a:1021114710076. PMID: 15348666.

10. de Bruijn JD, Bovell YP, Davies JE, van Blitterswijk CA. Osteoclastic resorption of calcium phosphates is potentiated in postosteogenic culture conditions. J Biomed Mater Res. 1994 Jan;28(1):105-12. doi: 10.1002/jbm.820280114. PMID: 8126021.

11. Carlisle EM. Silicon: a requirement in bone formation independent of vitamin D1. Calcif Tissue Int. 1981;33(1):27-34. doi: 10.1007/BF02409409. PMID: 6257332.

12. M. Sadat-Shojai, M.T. Khorasani, E. Dinpanah-Khoshdargi, A. Jamshidi, Synthesis methods for nanosized hydroxyapatite with diverse structures, Acta Biomater. 9(2013) 7591–7621.

13. Mohd Pu'ad NAS, Koshy P, Abdullah HZ, Idris MI, Lee TC. Syntheses of hydroxyapatite from natural sources. Heliyon. 2019 May 8;5(5):e01588.

14. Gibson IR, Best SM, Bonfield W. Chemical characterization of silicon-substituted hydroxyapatite. J Biomed Mater Res. 1999 Mar 15;44(4):422-8. doi: 10.1002/(sici)1097-4636(19990315)44:4<422::aid-jbm8>3.0.co;2-#. PMID: 10397946.

15. Coathup MJ, Samizadeh S, Fang YS, Buckland T, Hing KA, Blunn GW. The Osteoinductivity of Silicate-Substituted Calcium Phosphate. Journal of Bone and Joint Surgery-American Volume. 2011 Dec

7; 93A(23):2219–26. (doi: 10.2106/Jbjs.J.01623)

16. Patel N, Best SM, Bonfield W, Gibson IR, Hing KA, Damien E, et al. A comparative study on the in vivo behavior of hydroxyapatite and silicon substituted hydroxyapatite granules. J Mater Sci Mater Med. 2002 Dec; 13(12):1199–206. (5111124 [pii]) PMID: 15348666

17. Wiens M, Bausen M, Natalio F, Link T, Schlossmacher U, Muller WE. The role of the silicatein-alpha interactor silintaphin-1 in biomimetic biomineralization. Biomaterials. 2009 Mar; 30(8):1648–56. (S0142-9612(08)00979-4 [pii] doi: 10.1016/j.biomaterials.2008.12.021) PMID: 19118892

18. Rai A, Perry CC. Facile Fabrication of Uniform Silica Films with Tunable Physical Properties Using Silicatein Protein from Sponges. Langmuir. 2010 Mar 16; 26(6):4152–9. (doi: 10.1021/La903366a) PMID: 20000795

19. Botelho CM, Lopes MA, Gibson IR, Best SM, Santos JD. Structural analysis of Si-substituted hydroxyapatite: zeta potential and X-ray photoelectron spectroscopy. J Mater Sci Mater Med. 2002 Dec; 13 (12):1123–7. (5111106 [pii]) PMID: 15348653

20. Kalia P, Brooks RA, Kinrade SD, Morgan DJ, Brown AP, Rushton N, et al. (2016) Adsorption of Amorphous Silica Nanoparticles onto Hydroxyapatite Surfaces Differentially Alters Surfaces Properties and Adhesion of Human Osteoblast Cells. PLoS ONE 11 (2): e0144780. doi:10.1371/journal.pone.0144780

21. M. Borden, M. Attawia, Y. Khan, and C. T. Laurencin, "Tissue engineered microsphere-based matrices for bone repair: design and evaluation," Biomaterials, vol. 23, no. 2, pp. 551–559, 2002.

22. Hing, K.A., Revell, P.A., Smith, N. & Buckland, T. (2006) Effect of silicon level on rate, quality and progression of bone healing within silicate-substituted porous hydroxyapatite scaffolds. Biomaterials 27: 5014–5026.

23. Sych, E.E., Pinchuk, N.D., Klimenko, V.P. et al. Synthesis and Properties of Si-Modified Biogenic Hydroxyapatite Ceramics. Powder Metall Met Ceram 54, 67–73 (2015). https://doi.org/10.1007/s11106-015-9681-z

24. Ranna, Tolouei. Effect of Nano Silica On the Sinterability of Hydroxyapatite Dense Bodies. Trans Tech Publications, Switzerland, 2011.

25. Turner, I.G. Ceramics and Glasses. In Biomedical Materials; Narayanan, R., Ed.; Springer: New York, NY, USA, 2009; pp. 3–39.

26. Bowen, P.; Carry, C. From powders to sintered pieces, forming, transformations and sintering of nanostructured ceramic oxides. Powder Technol. 2002, 128, 248–255.

27. Liu, D.-M.; Lin, J.-T. Influence of ceramic powders of different characteristics on particle packing structure and sintering behavior. J. Mater. Sci. 1999, 34, 1959–1972.

28. Chaim, R.; Levin, M.; Shlayer, A.; Estournès, C. Sintering and densification of nanocrystalline ceramic oxide powders: A review. Adv. Appl. Ceram. Struct. Funct. Bioceram. J. Adv. Psychiatr. Treat. 2008, 107, 159–169.

29. Mosquim V, Ferrairo BM, Vertuan M, Magdalena AG, Fortulan CA, Lisboa-Filho PN, Cesar PF, Bonfante EA, Honório HM, Sanches Borges AF. Structural, chemical and optical characterizations of an experimental SiO2-Y-TZP ceramic produced by the uniaxial/isostatic pressing technique. J Mech Behav Biomed Mater. 2020 Jun;106:103749. doi: 10.1016/j.jmbbm.2020.103749. Epub 2020 Apr 1. PMID: 32250942.

30. Vallet-Regí M, Ragel CV, Salinas AJ. Glasses with medical applications. Eur J Inorg Chem 2003:1029–42.

31. Pereira MM, Hench LL. Mechanisms of hydroxyapatite formation on porous gel-silica substrates. J Sol–Gel Sci Technol 1996;7:59–68.

32. Xynos ID, Edgar AJ, Buttery LD, Hench LL, Polak JM. Gene-expression profiling of human osteoblasts following treatment with the ionic products of Bioglass 45S5 dissolution. J Biomed Mater Res 2001;55:151–7.

33. Bielby RC, Boccaccini AR, Polak JM, Buttery LD. In vitro differentiation and in vivo mineralization of osteogenic cells derived from human embryonic stem cells. Tissue Eng A 2004;10:1518–25.

34. Gorustovich A, Roether J, Boccaccini AR. Effect of bioactive glasses on angiogenesis: in-vitro and in-vivo evidence. Tissue Eng B Rev 2010;16:199–207.

35. Erbereli, Rogério. Avaliação da qualidade óssea de bovinos [dissertação]. São Carlos: Universidade de São Paulo, Bioengenharia; 2017 [citado 2020-10-27]. doi:10.11606/D.82.2018.tde-20082018-121530.

36. M.R. Ayatollahi, M.Y. Yahya, H.A. Shirazi, S.A. Hassan, Mechanical and tribological properties of hydroxyapatite nanoparticles extracted from natural bovine bone and the bone cement developed by nano-sized bovine hydroxyapatite filler, Ceram. Int. 41 (2015) 10818–10827.

37. Pires LA, de Azevedo Silva LJ, Ferrairo BM, Erbereli R, Lovo JFP, Ponce Gomes O, Rubo JH, Lisboa-Filho PN, Griggs JA, Fortulan CA, Borges AFS. Effects of ZnO/TiO2 nanoparticle and TiO2 nanotube additions to dense polycrystalline hydroxyapatite bioceramic from bovine bones. Dent Mater. 2020

38. Srinivasa RR, Saad AK. Shear-Thickening Response of Fumed Silica Suspensions under Steady and Oscillatory Shear. J. Colloid Interf. Sci. 185 (1997) 57–67.

39. Whitby, C. P., Krebsz, M., & Booty, S. J. (2018). Understanding the role of hydrogen bonding in the aggregation of fumed silica particles in triglyceride solvents. Journal of colloid and interface science, 527, 1-9.

40. Reghavan SR, Khan S.A. Shear-induced microstructural changes in flocculated suspensions of fumed silica, Journal of Rheology Volume 39, Issue 6, November 1995, Pages 1311-1325. DOI: 10.1122/1.550638

41. Yziquel F, Carreu PJ, Tanguy PA. Non-linear viscoelastic behavior of fumed silica suspensions. Rheol Acta 38: 14-25 (1999)

42. M.K. Herliansyah, D.A. Nasution, M. Hamdi, A. Ide-Ektessabi, M.W. Wildan, A.E. Tontowi, Preparation and characterization of natural hydroxyapatite: a comparative study of bovine bone hydroxyapatite and hydroxyapatite from calcite, Mater. Sci. Forum 561–565 (2007) 1441–1444.

43. C. Ooi, M. Hamdi, S. Ramesh, Properties of hydroxyapatite produced by annealing of bovine bone, Ceram. Int. 33 (2007) 1171–1177.

44. Loganathan, S.; Tikmani, M.; Ghoshal, A. K. Novel Pore- Expanded MCM-41 for CO2 Capture: Synthesis and Characterization. Langmuir 2013, 29, 3491−3499.

45. Cui, S.; Cheng, W. W.; Shen, X. D.; Fan, M. H.; Russell, A.; Wu, Z.; Yi, X. B. Mesoporous Amine-Modified SiO2 Aerogel: A Potential CO2 Sorbent. Energy Environ. Sci. 2011, 4, 2070−2074.

46. Kothapalli C, Wei M, Vasiliev A, Shaw MT. Influence of temperature and concentration on the sintering behavior and mechanical properties of hydroxyapatite. Acta Mater 2004;52:5655–63.

47. A. Boskey, N. P. Camacho, FT-IR imaging of native and tissue engineered bone and cartilage, Biomaterials 28(2007)2456–2478.

48. Kelly, J.R., Benetti, P., 2011. Ceramic materials in dentistry: historical evolution and current practice. Aust. Dent. J. 56, 84–96. https://doi.org/10.1111/j.1834-7819.2010.01299.x.

49. Baklouti, S., Bouaziz, J., Chartier, T., Baumard, J., 2001. Binder burnout and evolution of the mechanical strength of dry-pressed ceramics containing poly(vinyl acohol). J. Eur. Ceram. Soc. 21, 1087–1092. https://doi.org/10.1016/S0955-2219(00)
00305-8.

50. Borum L, Wilson OC. Surface modification of hydroxyapatite. Part II. Silica. Biomaterials. 2003 Sep;24(21):3681-8. doi: 10.1016/s0142-9612(03)00240-0. PMID: 12818539.

51. Hench LL, Wilson J. Surface-active biomaterials. Science. 1984 Nov 9;226(4675):630-6. doi: 10.1126/science.6093253. PMID: 6093253.

52. Polymer Properties Database. polymerdatabase.com

53. Jiang, L., Liao, Y., Wan, Q., Li, W., 2011. Effects of sintering temperature and particle size on the translucency of zirconium dioxide dental ceramic. J. Mater. Sci. Mater. Med. 22, 2429–2435. https://doi.org/10.1007/s10856-011-4438-9.

54. Pizette, P., Martin, C.L., Delette, G., Sans, F., Geneves, T., 2013. Green strength of binder-free ceramics. J. Eur. Ceram. Soc. 33, 975–984. https://doi.org/10.1016/j.jeurceramsoc.2012.11.018.

55. Sigma-Aldrich Product Information. Silica, Fumed. 2012 Sigma-Aldrich Co.

56. Barraclough, K.G., Loni, A., Caffull, E., Canham, L.T., 2007. Cold compaction of silicon powders without a binding agent. Mater. Lett. 61, 485–487. https://doi.org/
10.1016/j.matlet.2006.04.102.

57. A. Royer, J. Viguie, M. Heughebaert, J. Heughebaert, Stoichiometry of hydroxyapatite: influence on the flexural strength, J.Mater. Sci:Mater. Med. 4(1993)76–82.

58. P.E. Wang, T. Chaki, Sintering behaviour and mechanical properties of hydroxyapatite and dicalcium phosphate, J.Mater. Sci:Mater.Med.4 (1993) 150–158.

59. M. Jarcho, C. Bolen, M. Thomas, J. Bobick, J. Kay, R. H. Doremus, Hydroxylapatite synthesis and characterization in dense polycrystalline form, J.Mater.Sci.11(1976)2027–2035.

60. Sanati, M., Andersson, A., 1993. DRIFT study of the oxidation and the ammoxidation of toluene over a TiO2 (B) -supported vanadia catalyst. J. Mol. Catal. 81, 51–62. https://doi.org/10.1016/0304-5102(93)80022-M.

61. Ishikawa T, Wakamura M, Kondo S. Surface characterization of calcium hydroxyapatite by Fourier transform infrared spectroscopy. Langmuir 1989;5:140.

62. Gadaleta SJ, Paschalis EP, Betts F, Mendelsohn R, Boskey AL. Fourier transform infrared spectroscopy of the solution-mediated conversion of amorphous calcium phosphate to

hydroxyapatite: new correlations between X-ray diffraction and infrared data. Calcif Tissue Int 1996;58:9.

63. Rey C, Shimizu M, Collins B, Glimcher MJ.Resolut ion-enhanced Fourier transform infrared spectroscopy study of the environment of phosphate ion in the early deposits of a solid phase calcium phosphate in bone and enamel and their evolution with age: 2.Investigations in the n3 PO4 domain.Calcif Tissue Int 1991;49:383.

64. L. Borum, O.C. Wilson Jr. / Biomaterials 24 (2003) 3681–3688

65. Socrates G. Infrared and Raman characteristic group frequencies: tables and charts.New York: Wiley, 2001. p.229–46.

66. Szepesi CJ, Cantonnet J, Kimel RA, Adair JH. A critical assessment of nanometer scale zirconia green body formation by pressure filtration and uniaxial compaction. J Am Ceram Soc 2011;29(29390):2011.

67. A.K. Dhaliwal, J.N.Hay. The characterization of polyvinyl butyral by thermal analysis. Thermochimica Acta. Volume 391, Issues 1–2, 12 August 2002, Pages 245-255. https://doi.org/10.1016/S0040-6031(02)00187-9

68. N.M.S. El-Din, and M.W. Sabaa, Polym. Degrad. Stabil., 47, 283 (1995).

69. Kuscer D, Bakarič T, Kozlevčar B, Kosec M. Interactions between lead-zirconate titanate, polyacrylic acid, and polyvinyl butyral in ethanol and their influence on electrophoretic deposition behavior. J Phys Chem B. 2013 Feb 14;117(6):1651-9. doi: 10.1021/jp305289u. Epub 2012 Oct 22. PMID: 23025567.

70. Kruse A, Jung RE, Nicholls F, Zwahlen RA, Ha¨mmerle CHF, Weber FE. Bone regeneration in the presence of a synthetic hydroxyapatite/silica oxide -based and a xenogenic hydroxyapatite -based bone substitute material. Clin. Oral Impl. Res. 22, 2011; 506–511. doi: 10.1111/j.1600-0501.2010.02039.x

71. Xu, J.L. & Khor, K.A. (2007) Chemical analysis of silica doped hydroxyapatite biomaterials consolidated by a spark plasma sintering method. Journal of Inorganic Biochemistry 101: 187–195.

72. Seaborn, C.D. & Nielsen, F.H. (2002) Silicon deprivation decreases collagen formation in wounds and bone, and ornithine transaminase enzyme activity in liver. Biological Trace Element Research 89: 247–258.

73. Patel, N., Brooks, R.A., Clarke, M.T., Lee, P.M., Rushton, N., Gibson, I.R., Best, S.M. & Bonfield, W. (2005) In vivo assessment of hydroxyapatite and silicate-substituted hydroxyapatite granules using an ovine defect model. Journal of Material Science. Materials in Medicine 16: 429–440.

78. Huang, D.M., Chung, T.H., Hung, Y., Lu, F., Wu, S.H., Mou, C.Y., Yao, M. & Chen, Y.C. (2008) Internalization of mesoporous silica nanoparticles induces transient but not sufficient osteogenic signals in human mesenchymal stem cells. Toxicology and Applied Pharmacology 231: 208–215.

79. Werner, J., Linner-Krcmar, B., Friess, W. & Greil, P. (2002) Mechanical properties and in vitro cell compatibility of hydroxyapatite ceramics with graded pore structure. Biomaterials 23: 4285–4294.

80. M. O. Prado, M. L. F. Nascimento, E. D. Zanotto. (2008). On the sinterability of crystallizing glass powders," J. Non-Cryst. Solids, 354[40-41] 4589-97.

81. M. O. Prado, E. D. Zanotto. (2002). "Glass sintering with concurrent crystallization," C. R. Chim., 5[11] 773-86.

82. Al-Hasnawi, Ahmed Ali Kadhim, & Al-Hydary, Imad Ali Disher. (2019). The devitrification kinetics of transparent silica glass prepared by gel-casting method. Matéria (Rio de Janeiro), 24(1), e-12317. Epub May 20, 2019.

83. D. Wei, R. Dave, R. Pfeffer, Mixing and characterization of nanosized powders: an assessment of different techniques, J. Nanopart. Res. 4 (2002) 21–41.

3 FUNDAMENTED DISCUSSION

3 FUNDAMENTED DISCUSSION

The great demand for HA, especially in nanometric proportions, motivates scientific investigations and justifies the search for sustainable and low-cost appeal. Natural HA, usually extracted from biological sources or waste, meets this demand and even has superior structural characteristics compared to synthetic HA [MOHD PU'AD *et al.*, 2019]. In the present studies, cortical part of femoral bovine bone was used because of morphologically and structurally similarity to human bone [HERLIANSYAH *et al.*, 2007]. Based on literature demand for further investigations and considering processing aspects and characteristics of the powder [SADAT-SHOJAI *et al.*, 2013], two nanoparticulation methods were elected to appraisal.

Sonochemical and mechanochemical ball mill methods are classified as inexpensive and do not require many chemical reagents for processing [SADAT-SHOJAI *et al.*, 2013]. However, the morphology and crystallinity of the obtained powder is variable, further studies and a precise methodology description are necessary toward providing greater predictability. Both methodologies have proved to be effective in decreasing nanometer-sized the particles of bovine HA, since the sonochemical and milling methods reached an average of 60 nm and 40 nm, respectively. In order to evaluate the physical-chemical characteristics of the products obtained, a series of tests were executed.

XDR provide the phases identification and comparison before and after the methods. The resulting diffractograms demonstrates an accordance with reported descriptions for bovine origin HA (XDR JCPDS file no. 9-432, 1996) [JCPDS, 1996] and with pure HA phase (211, 300, 202 diffraction peaks) [AYATOLLAHI *et al.*, 2015], which demonstrates the great performance of the methods, without degradation of the particles and with similarity to the described patterns. Dihydroxylation of HA had occurred and is evidenced at diffractogram (211 peak) [KUSRINI; SONTANG, 2012], which make the materials good candidates for bone substitutes. EDX is an elemental analysis technique and allowed to confirm the presence of Ca, P, O, and minor elements (Mg^{2+} and Na^{+}), also relevant to optimize the bone substitute function [HERLIANSYAH *et al.*, 2007]. Generally, most literature have reported Ca/P ratio 1.67 as the most effective in promoting bone regeneration [AKRAM *et al.*, 2013], but the range of ≅ 1.92 was obtained with the methodologies performed and still belongs to an acceptable range [JOSCHEK; NIES; KROTZ; OPFERICH, 2000; OOI; HAMDI; RAMESH, 2007].

The FTIR spectrum provides a characteristic "molecular fingerprint" that can be used to display, scan and identify organic and inorganic samples. The representativeness of the bands was described in the respective image. Phosphate ions appeared in the spectrum on v1 (965 cm^{-1}), v3 (1100 – 1035 cm^{-1}), and v4 mode (633, 603 and 565 cm^{-1} bands). Carbonate ions arises with v2 (873 – 880 cm^{-1} - out-of-plane bend vibration) and v3 (1400 – 1600 cm^{-1}) mode and could be associated with impurity as residual organic component after calcination [DOROZHKIN, 2010]. TEM images provided the measurement and the identification of the nanoflakes particles conformation [AYATOLLAHI *et al.*, 2015], agreeing with the expected result for HA of biogenic source and obtained by association of procedures [SADAT-SHOJAI *et al.*, 2013; MOHD PU'AD *et al.*, 2020; MOSTAFA, 2005]. The association of calcination and sonochemical/ball mill provides promising results of reaction kinetics, reduction of particle size and high purity.

Although the two nanoparticulation methods were effective and produced particles with structural and chemical characteristics suitable for biomedical use, the study of synthetization an experimental SiO_2/nano-hydroxyapatite composite ceramic opted for particles produced by the ball mill mechanochemical method. Associate nano-HA and fumed silica has intention of having a larger area available for interaction and, since the alcoholic medium was used for mixture on gyratory ball mill, this conjunction with a polar organic solvents tends to promote a dispersion to mechanical stress [SRINIVASA; SAAD, 1997] and form a viscous liquid favorable for the method elected [SRINIVASA; SAAD, 1997; SCHWARZ; MILNE, 1972].

Three essential factors were considered in the study of structural and chemical evaluation of an experimental ceramic: percentage of material and binder added to the matrix and firing temperature. Following a characterization protocol similar to the analysis of nanoparticulation methods, differing only in the type of microscopy (TEM / SEM), it was possible to thoroughly analyze the results obtained. As the concentration of HA increased, the SEM images made it possible to identify an increase in the incidence and volume of the pores. Compression failures and a non-uniform distribution of HA may explain these findings [PRAKASAM *et al.*, 2015]. At 1200 °C the SH composite ceramic with 5% and 10% of HA presents filaments within the ceramic bulk, more evident at 10% group. According to EDX their composition is mostly magnesium. As already discussed, magnesium is a favorable trace element for biomaterial, however further investigations should be performed to elucidate the reason of this formation [HERLIANSYAH *et al.*, 2007]. FTIR pattern demonstrate that for

concentrations of 3 and 10% HA, according to the sintering temperature, the bands of CO_2 became more prominent, while for the concentration of 5% this relationship was reversed.

Evaluating two proportions of PVB provided not only easiness during the conformation stages of the specimens, but also an important structural observation of the material. Although the mechanical characteristic is relevant in dense ceramics and, in this respect, less pore incrustation is unfavorable [MICHELSEN *et al.*, 2008; SRINIVASA; SAAD, 1997], other clinical applications may arise requiring greater porosity to favor cell adhesion or even the penetration of widely distributed drugs. The complete elimination of binder is 600 – 700 °C [AYATOLLAHI *et al.*, 2015]. For this reason, EDX only demonstrates a slight increase in carbon levels on 2.4 wt.% of PVB group. SEM images shows fewer pores at groups with higher concentration of PVB, while cracks could be visualized at SH composite ceramic with 3% of HA with both concentrations of binder, and 10% with 2.4 wt.% of PVB. According to the XDR and FTIR analysis, it can be observed that the use of 1.2% or 2.4 wt.% of PVB did not influence the physicochemical characteristics of the experimental material, which suggests complete burn out. However, a higher concentration seems to have contributed to a more effective compaction of the green-body specimens, providing a lower incidence of cracks and apparent pores.

The sintering temperature varied among 1100, 1200 and 1300 °C, following the same slow scheme. For concentrations of 3 and 10% HA, according to the sintering temperature, the FTIR bands of CO_2 became more prominent, while for the concentration of 5% this relationship was reversed. XDR patter of 1100 °C samples presented an attempt of binding with substantial increase in FWHM. At 1200°C the peaks were evidenced and at 1300 °C the degradation already prevented its increase, the HA peaks start to disappear and the formation of $Ca(OH)_2$ peaks are promoted. This evolution that occurs with the increase in temperature can be confirmed by the SEM images. At 1100 °C sample, although compacted, the flaking aspects of the agglomerated fumed silica continues to be observed at higher magnifications. At samples of 1200 °C and 1300 °C the matrix is more homogeneous, with union of particles. However, the pores of the highest temperature appear to be of greater volume and filaments, already described, are present at 1200 °C sample. From the results obtained and the temperatures tested, the 1200 °C plateau proved to be the most suitable for SH composite ceramic with HA. However, it is suggested that the thermogravimetric analysis (TGA) of the material be carried out so that through the monitoring of sample loss and / or mass gain as a function of time or temperature, it is possible to establish both a specific sintering scheme and the definition of the temperature of the plateau [CHARSLEY; WARRINGTON, 1991].

Within the limitations of the study, it can be concluded that the uniaxial/isostatic powder compression is an efficient method to obtain SH composite ceramic. The temperature of 1200 °C presented potentialized chemical bonds without the degradation of HA at XDR profile, SEM images suggests that 2.4 wt.% of PVB result in optimized compaction and a lower incidence of cracks and pores, which should be investigated using additional supporting methods, and the SH composite ceramic with 5% of HA presents potential superior properties to biomaterial.

The path of making an experimental biomaterial is long and goes through countless variations and evaluations until it presents the ideal characteristics for clinical use. However, while in the past trial and error were the principal alternatives for the design of new biomaterials, current studies of the structure and chemical characteristics can give greater support to innovations [OLADEJI; UMORU; ARIBO, 2012]. Biomaterials research represents one of the most important fields of modern medicine and dentistry and it is responsibility of the scientific community to bring together the various expertise for the benefit of potential users.

4 CONCLUSIONS

4 CONCLUSIONS

Within the limitations of the studies, it can be concluded that sonication (≅ 60 nm) and ball mill (≅ 40 nm) methods, associated with prior calcination, were capable of producing nanosized bovine HA particles, manteining an appropriate stoichiometry, morphology and purity. According to SH composite ceramic, the uniaxial/isostatic powder compression is an efficient method. The temperature of 1200 °C presented potentialized chemical bonds without the degradation of HA at XDR profile, SEM images suggests that 2.4 wt.% of PVB result in optimized compaction and a lower incidence of cracks and pores, and the SH composite ceramic with 5% of HA presents potential superior properties to biomaterial. Further studies with different sintering temperatures, thermogravimetric analysis, and different HA concentrations are needed to reach the maximum potential of the experimental material.

REFERENCES

REFERENCES

AKRAM, M. *et al.* Extracting hydroxyapatite and its precursors from natural resources. **Journal of Materials Science**, v. 49, p. 1461–1475, nov. 2013.

AYATOLLAHI, M.R. *et al.* Mechanical and tribological properties of hydroxyapatite nanoparticles extracted from natural bovine bone and the bone cement developed by nano-sized bovine hydroxyapatite filler. **Ceramics International**, v. 41, issue 9, part A, p. 10818–10827, nov. 2015.

BEST, S.M. *et al.* **Silicon-substituted apatites and process for the preparation thereof.** Depositante: U.S. Patent No. 6,312,468. Depósito: 6 Nov. 2001.

BORDEA, I.R. *et al.* Nano-hydroxyapatite use in dentistry: a systematic review. **Drug Metabolism Reviews**, v. 52, issue 2, may 2020.

BOSE, S. *et al.* Synthesis, Processing, Mechanical, and Biological Property Characterization of Hydroxyapatite Whisker-Reinforced Hydroxyapatite Composites. **Journal of the American Ceramic Society**, v. 92, issue 2, feb. 2009.

BOSKEY, A.L. Natural and Synthetic Hydroxyapatites. In: Ratner, B. et al. (org.). **Biomaterials Science: An introduction to materials in medicine**. Third Edit, Elsevier, 2013.

BOWEN, P.; CARRY, C. From powders to sintered pieces, forming, transformations and sintering of nanostructured ceramic oxides. **Powder Technology**, v. 128, issues 2-3, p. 248-255, dec. 2002.

BRANDON, D.; KAPLAN, W.D. Microstructural characterization of materials. **John Wiley & Sons**, feb. 2013.

CAI, Y. *et al.* Role of hydroxyapatite nanoparticle size in bone cell proliferation. **Journal of Materials Chemistry**, v. 17, n. 36, p. 3780-3787, june 2007.

CAO, L.; ZHANG, C.; HUANG, J. Synthesis of hydroxyapatite nanoparticles in ultrasonic precipitation. **Ceramics International**, v. 31, issue 8, p. 1041-1044, 2005.

CARLISLE, E.M. Silicon: an essential element for the chick. **Science**, v. 178, issue 4061, p. 619-621, nov. 1972.

CHARSLEY, E. L.; WARRINGTON, S. B. **Thermal Analysis: Techniques & Applications**. Leeds: Royal Society of Chemistry, 1991, 296p.

DE JONG, W.F. La substance minérale dans les os, **Recueil des Travaux Chimiques des Pays-Bas,** v. 45, n. 6, pp. 445–448, apr. 1926.

DENISSEN, H. W. *et al*. Eleven-year study of hydroxyapatite implants. **Journal of Prosthetic Dentistry** v. 61, issue 6, p. 706–712, june 1989.

DOREMUS, R.H. Review – Bioceramics. **Journal of Materials Science**, vol. 27, no. 2, pp. 285–297, 1992.

DOROZHKIN, S.V. Nanosized and nanocrystalline calcium orthophosphates. **Acta Biomaterialia**, v. 6, issue 3, p. 715-734, mar. 2010.

DSM, A Brief History of Biomedical Materials, **Corporate Communications**, 2009. Disponível em: http://www.dsm.com/en US/cworld/public/medical downloads/. Acesso em: 5 Nov. 2020.

FU, L.-H. *et al.* Microwave assisted hydrothermal synthesis of cellulose/hydroxyapatite nanocomposites. **Polymers**, vol. 8 (9), p. 316., sept. 2016.

FULLER, C.C. *et al.* Mechanisms of uranium interactions with hydroxyapatite: implications for groundwater remediation. **Environmental Science & Technology**, v. 36, n. 2, p. 158–165, jan. 2002.

GIARDINA, M.A.; FANOVICH, M.A. Synthesis of nanocrystalline hydroxyapatite from Ca(OH)2 and H3PO4 assisted by ultrasonic irradiation. **Ceramics International**, v. 36, issue 6, p. 1961-1969, aug. 2010.

GIBSON, I.R.; BEST, S.M.; BONFIELD, W. Chemical characterization of silicon-substituted hydroxyapatite. **Journal of Biomedical Materials Research**, v. 44, issue 4, jan. 1999.

HENCH, L.; POLAK, J. Third generation biomedical materials. **Science**, v. 8, n. 295(5557), p. 1014-7, feb. 2002.

HENCH, L.L.; CLARKE, A.E. **Biocompatibility of Orthopaedic Implants**. In: WILLIAMS, D.F. (org.). CRC Press, Inc., 1982. cap. 6.

HERLIANSYAH, M.K. *et al.* Preparation and characterization of natural hydroxyapatite: a comparative study of bovine bone hydroxyapatite and hydroxyapatite from calcite, **Materials Science Forum**, V. 561-565, p. 1441-1444, oct. 2007.

HONARMANDI, P. *et al.* Milling media effects on synthesis, morphology and structural characteristics of single crystal hydroxyapatite nanoparticles. **Advances in Applied Ceramics**, v. 109, issue 2, p. 117-122, feb. 2010.

IBRAHIM, M. *et al.* Hydroxyapatite, a multifunctional material for air, water and soil pollution control: A review. **Journal of Hazardous Materials**, v. 383, n. 5, feb. 2020.

JCPDS Card File No. 9-432 (Hydroxyapatite), 1996. **Joint Committee on Powder Diffraction Standards.** Swathmore, PA.

JEVTIC, M. *et al.* Crystal structure of hydroxyapatite nanorods synthesized by sonochemical homogeneous precipitation. **Crystal Growth & Design**, v. 8, n. 7, p. 2217-2222, june 2008.

JIANG, L.; LIAO, Y.; WAN, Q.; LI, W. Effects of sintering temperature and particle size on the translucency of zirconium dioxide dental ceramic. **Journal of Materials Science: Materials in Medicine**, v. 22, p. 2429–2435, sept. 2011.

JOSCHEK, S.; NIES, B.; KROTZ, R.G.; OPFERICH, A. Chemical and physicochemical characterization of porous hydroxyapatite ceramics made of natural bone. **Biomaterials**, v. 21, p. 1645–1658, aug. 2000.

KRAJEWSKI, A. *et al.* Spectrometric study of the thermal evolution of mechanochemically prepared hydroxyapatite-based powders. **Crystal Research and Technology**, v. 31, issue 5, p. 637–46, 1996.

KRUSE, A. *et al.* Bone regeneration in the presence of a synthetic hydroxyapatite/silica oxide-based and a xenogenic hydroxyapatite-based bone substitute material. **Clinical Oral Implants Research**, v. 22(5), p. 506-511, may 2011.

KUSRINI, E.; SONTANG, M. Characterization of x-ray diffraction and electron spin resonance: Effects of sintering time and temperature on bovine hydroxyapatite. **Radiation Physics and Chemistry**, v. 81, issue 2, p. 118-125, feb. 2012.

LIU, D.-M.; LIN, J.-T. Influence of ceramic powders of different characteristics on particle packing structure and sintering behavior. **Journal of Materials Science**, v. 34, p. 1959–1972, apr. 1999.

MICHELSEN, V.B. *et al.* Quantitative analysis of TEGDMA and HEMA eluted into saliva from two dental composites by use of GC/MS and tailor-made internal standards. **Dental Materials**, v. 24, issue 6, p. 724-731, june 2008.

MOHD PU'AD, N.A.S. *et al.* Syntheses of hydroxyapatite from natural sources. **Heliyon**. v.8;5(5), e01588, may 2019. DOI 10.1016/j.heliyon.2019.e01588. Disponível em: https://doi.org/10.1016/j.heliyon.2019.e01588. Acesso em: 5 Nov. 2020.

MONDAL, S.; DOROZHKIN, S.V.; PAL, U. Recent progress on fabrication and drug delivery applications of nanostructured hydroxyapatite. **Wiley Interdisciplinary Reviews - Nanomedicine Nanobiotechnology**, v. 10, n. 4, e1504, jul. 2018. DOI 10.1002/wnan.1504. Disponível em: https://doi.org/10.1002/wnan.1504. Acesso em: 5 nov. 2020.

MOSTAFA, N.Y. Characterization, thermal stability and sintering of hydroxyapatite powders prepared by different routes. **Materials Chemistry and Physics**, v. 94, issues 2-3, p. 333–41, dec. 2005.

NASIRI-TABRIZI, B.; HONARMANDI, P.; EBRAHIMI-KAHRIZSANGI, R., Synthesis of nanosize single-crystal hydroxyapatite via mechanochemical method. **Materials Letters**, v. 63, issue 5, p. 543-546, feb. 2009.

OLADEJI, O.I.; UMORU, L.E.; ARIBO, S. Natural Products: A Minefield of Biomaterials. **International Scholarly Research Notices**, vol. 2012, Article ID 983062, 20 pages, 2012. DOI 10.5402/2012/983062. Disponível em: https://doi.org/10.5402/2012/983062. Acesso em: 5 nov. 2020.

OOI, C.Y.; HAMDI, M.; RAMESH, S. Properties of hydroxyapatite produced by annealing of bovine bone. **Ceramics International**, v. 33, issue 7, p. 1171–1177, sept. 2007.

PATEL, N. *et al.* A comparative study on the in vivo behavior of hydroxyapatite and silicon substituted hydroxyapatite granules. **Journal of Materials Science: Materials in Medicine**, v. 13(12), p. 1199–1206, dec. 2002.

PIZETTE, P. *et al.* Green strength of binder-free ceramics. **Journal of the European Ceramic Society**, v. 33, p. 975–984, may 2013.

PRAKASAM, M. *et al.* Fabrication, Properties and Applications of Dense Hydroxyapatite: A Review. **Journal of Functional Biomaterials**, v. 6, n. 4 p. 1099-140, dec. 2015.

REGHAVAN, S.R.; KHAN, S.A. Shear-induced microstructural changes in flocculated suspensions of fumed silica, **Journal of Rheology**, v. 39, issue 6, p. 1311-1325, nov. 1995.

ROUHANI, P.; TAGHAVINIA, N.; ROUHANI, S. Rapid growth of hydroxyapatite nanoparticles using ultrasonic irradiation. **Ultrasonics Sonochemistry**, v. 17, issue 5, p. 853-856, june 2010.

RUKSUDJARIT, A. *et al.* Synthesis and characterization of nanocrystalline hydroxyapatite from natural bovine bone. **Current Applied Physics**, v. 8, issues 3-4, p. 270–272, may 2008.

SADAT-SHOJAI, M. *et al.* Synthesis methods for nanosized hydroxyapatite with diverse structures. **Acta Biomaterialia**, v. 9, p. 7591–7621, aug. 2013.

SCHWARZ, K.; MILNE, D.B. Growth-promoting effects of silicon in rats. **Nature**, v. 239, n. 5371, p. 333-334, oct. 1972.

SRINIVASA, R.R.; SAAD, A.K. Shear-Thickening Response of Fumed Silica Suspensions under Steady and Oscillatory Shear. **Journal of Colloid Interface Science**, v. 185, issue 1, p. 57–67, jan. 1997.

SZCZE, A.; HO, L.; CHIBOWSKI, E. Synthesis of hydroxyapatite for biomedical applications. **Advances in Colloid and Interface Science**, v. 249, p. 1-10, 2017.

TURNER, I.G. Ceramics and Glasses. In **Biomedical Materials**; Narayanan, R., Ed.; Springer: New York, NY, USA, 2009; pp. 3–39.

VALLET-REGÍ, M.; GONZÁLEZ-CALBET, J.M. Calcium phosphates as substitution of bone tissues. **Progress in Solid State Chemistry**, v. 32, issues 1-2, p. 1-31, 2004.

VON RECUM, A.F.; LABERGE, M. Educational goals for biomaterials science and engineering: prospective view. **Journal of Applied Biomaterials**, vol. 6, no. 2, pp. 137–144, 1995.

WANG, Y.; CHOU, S.; ZHANG, Z. Nanomaterials Innovation. **Small**, v. 15, n. 32, p. 1902246, aug. 2019.

WANG, Y.; LIU, L.; GUO, S. Characterization of biodegradable and cytocompatible nano-hydroxyapatite/polycaprolactone porous scaffolds in degradation in vitro. **Polymer Degradation and Stability**, v. 95, issue 2, p. 207-213, feb. 2010.

YEONG, K.; WANG, J.; NG, S.C. Mechanochemical synthesis of nanocrystalline hydroxyapatite from CaO and CaHPO4. **Biomaterials**, v. 22, issue 20, p. 2705-2712, oct. 2001.

ZHOU, H. ; LEE, J. Nanoscale hydroxyapatite particles for bone tissue engineering. **Acta Biomateralia**, v. 7, n. 7, pp. 2769-2781, july 2011.